NATIONAL BUREAU OF STANDARDS REPORT

9894

DEVELOPMENT OF A STABLE ULTRAVIOLET SOURCE AND TECHNIQUES FOR ACCURATE RADIOMETRY

Final Report to the
National Aeronautics and Space Administration
Order Number C-91488-A

U.S. DEPARTMENT OF COMMERCE
NATIONAL BUREAU OF STANDARDS

NATIONAL BUREAU OF STANDARDS

The National Bureau of Standards[1] was established by an act of Congress March 3, 1901. Today, in addition to serving as the Nation's central measurement laboratory, the Bureau is a principal focal point in the Federal Government for assuring maximum application of the physical and engineering sciences to the advancement of technology in industry and commerce. To this end the Bureau conducts research and provides central national services in three broad program areas and provides central national services in a fourth. These are: (1) basic measurements and standards, (2) materials measurements and standards, (3) technological measurements and standards, and (4) transfer of technology.

The Bureau comprises the Institute for Basic Standards, the Institute for Materials Research, the Institute for Applied Technology, and the Center for Radiation Research.

THE INSTITUTE FOR BASIC STANDARDS provides the central basis within the United States of a complete and consistent system of physical measurement, coordinates that system with the measurement systems of other nations, and furnishes essential services leading to accurate and uniform physical measurements throughout the Nation's scientific community, industry, and commerce. The Institute consists of an Office of Standard Reference Data and a group of divisions organized by the following areas of science and engineering:

Applied Mathematics—Electricity—Metrology—Mechanics—Heat—Atomic Physics—Cryogenics[2]—Radio Physics[2]—Radio Engineering[2]—Astrophysics[2]—Time and Frequency.[2]

THE INSTITUTE FOR MATERIALS RESEARCH conducts materials research leading to methods, standards of measurement, and data needed by industry, commerce, educational institutions, and government. The Institute also provides advisory and research services to other government agencies. The Institute consists of an Office of Standard Reference Materials and a group of divisions organized by the following areas of materials research:

Analytical Chemistry—Polymers—Metallurgy — Inorganic Materials — Physical Chemistry.

THE INSTITUTE FOR APPLIED TECHNOLOGY provides for the creation of appropriate opportunities for the use and application of technology within the Federal Government and within the civilian sector of American industry. The primary functions of the Institute may be broadly classified as programs relating to technological measurements and standards and techniques for the transfer of technology. The Institute consists of a Clearinghouse for Scientific and Technical Information,[3] a Center for Computer Sciences and Technology, and a group of technical divisions and offices organized by the following fields of technology:

Building Research—Electronic Instrumentation — Technical Analysis — Product Evaluation—Invention and Innovation— Weights and Measures — Engineering Standards—Vehicle Systems Research.

THE CENTER FOR RADIATION RESEARCH engages in research, measurement, and application of radiation to the solution of Bureau mission problems and the problems of other agencies and institutions. The Center for Radiation Research consists of the following divisions:

Reactor Radiation—Linac Radiation—Applied Radiation—Nuclear Radiation.

---

[1] Headquarters and Laboratories at Gaithersburg, Maryland, unless otherwise noted; mailing address Washington, D. C. 20234.
[2] Located at Boulder, Colorado 80302.
[3] Located at 5285 Port Royal Road, Springfield, Virginia 22151.

NATIONAL BUREAU OF STANDARDS REPORT

NBS PROJECT		NBS REPORT
2210417	July 1, 1966 - June 30, 1968	9894

DEVELOPMENT OF A STABLE ULTRAVIOLET SOURCE AND TECHNIQUES FOR ACCURATE RADIOMETRY

by

Henry J. Kostkowski
Albert T. Hattenburg

Final Report to the
National Aeronautics and Space Administration
Order Number C-91488-A

U.S. DEPARTMENT OF COMMERCE

NATIONAL BUREAU OF STANDARDS

PREFACE

The current report presents the work completed during the last two years on the project entitled "Development of a Stable Ultraviolet Radiant Source and Techniques for Accurate Radiometry".

Part I of the report is a tutorial paper on the calibration of a spectroradiometer for the purpose of measuring spectral radiance, spectral irradiance or spectral line intensities. The treatment includes detailed discussions on the radiation parameters, the slit function, available standards, and effects due to non-uniform targets, scattering and polarization. Though rigorous, it is presented at a level that requires only an elementary knowledge of optics and calculus.

Part II presents the work completed during the last two years on the use of the high pressure argon arc as a standard of ultraviolet radiance and irradiance. Earlier NBS Reports, numbers 8664 and 9099, incorporate work performed from January 1964 to December 1965 on the design, construction and preliminary measurements of this arc. The current report presents final results on the arc's operation, stability and calibration in terms of spectral radiance. Though the arc appears extremely useful as a spectral irradiance standard, only preliminary measurements were possible on this radiation parameter. New techniques and instrumentation are required before accurate (few percent) spectral irradiance measurements between 300 and 210 nm can be made. Work in this area will be initiated as soon as possible.

TABLE OF CONTENTS

Table of Contents, Continued

PART I

THE PRINCIPLES AND METHODS OF CALIBRATING SPECTRORADIOMETERS

H. J. Kostkowski

INTRODUCTION

This report introduces physical concepts and develops methods useful for accurately calibrating spectroradiometers for the purpose of determining the spectral radiance, irradiance or spectral line intensity of a source or beam of incoherent optical radiation. Though very little of the report is new, a complete, detailed treatment of this problem is not available in the literature, at least not to the author's knowledge. A spectroscopist or radiometrist is required to develop much of this material himself. With the number of people active in optical radiation measurements increasing and the number of graduate students in optics decreasing, it was considered worthwhile to write a tutorial type report on this subject.

In order to reach as broad an audience as possible, the level and pace of the presentation has been aimed at an individual familiar with relatively simple optics and calculus. However, it is hoped that some parts of the presentation will be sufficiently novel or thought provoking to also be of interest to the expert.

The approach and the methods described have evolved over a period of time from attempts to perform various types of calibrations useful in spectroscopy, pyrometry and radiometry. Discussions with colleagues and perusal of the literature have certainly contributed to this evolution. When the origin of a particular idea is known, its source is

certainly given. However, no attempt has been made to provide a complete bibliography on the subject, and if proper credit is not given, it is not intentional. Many of us have "invented" or "discovered" things that we later find have been used, known or even published previously.

There are two concepts that are very useful in dealing with the problems associated with accurate spectrometer calibrations. The first is the characterization or association of an optical ray with a particular radiation parameter called spectral radiance. The second is describing the spectral band pass of the spectrometer by the so-called slit or apparatus function. In the first section of this report spectral radiance is defined and the relation between the output and input of the spectrometer developed. In doing this, the need for the slit function arises and it is introduced and discussed in the second section. Applications of various types of calibrations when determining spectral radiance, line intensities, or irradiance, are presented in the remaining sections.

SPECTRAL RADIANCE

In order to characterize an arbitrary distribution of radiation; whether it is emanating from a source, propagating in space, or falling on the surface of a detector; it is convenient to have a quantity which describes the radiant power as a function of position and direction.

Since the radiant field is considered to be continuous in its distribution in space, a finite amount of radiant power cannot be propagated through a point or in a particular direction. However, it is still possible, through the use of a limiting process, to associate a quantity of radiant power with a point and a direction.

Consider an arbitrary incoherent radiant field represented in Fig. 1.

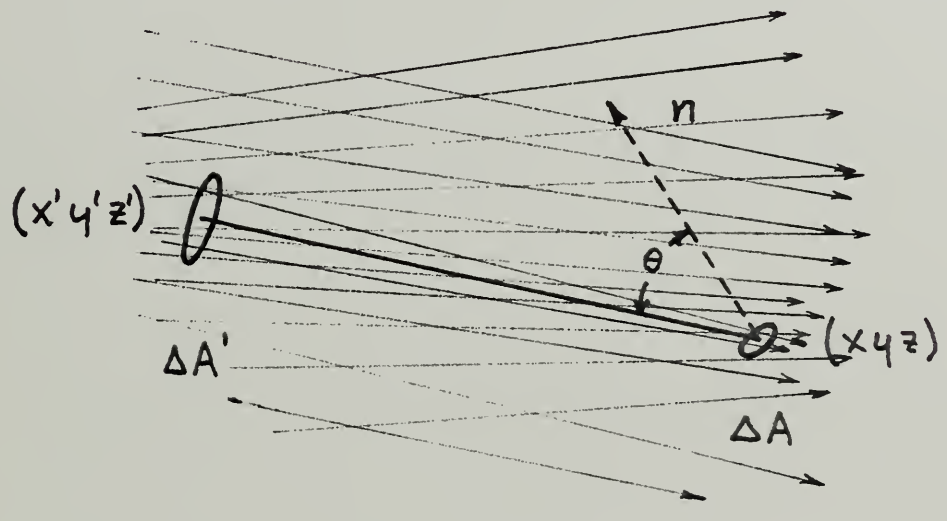

Fig. 1

by optical rays making arbitrary angles with the plane areas ΔA and ΔA' at the points (xyz) and (x'y'z') respectively. Call $\Delta_A\Phi$ the radiant energy passing through ΔA per unit time, often referred to as the radiant flux through ΔA, $\Delta_{A'}(\Delta_A\Phi)$ that portion of $\Delta_A\Phi$ also passing through ΔA'; and $\Delta_\lambda[\Delta_{A'}(\Delta_A\Phi)]$ that portion of $\Delta_{A'}(\Delta_A\Phi)$ contained in the wavelength

interval $\Delta\lambda$ surrounding the wavelength λ. The angle θ is the angle between the ray $(x'y'z') \rightarrow (xyz)$ and the normal to the ΔA surface. The limit of the ratio of the flux $\Delta_\lambda[\Delta_{A'}(\Delta_A\Phi)]$ to the product of $\Delta A\cos\theta$, $\Delta\Omega$ and $\Delta\lambda$, where $\Delta\Omega$ is the solid angle which is subtended by $\Delta A'$ and has its apex at the point (xyz), as ΔA, $\Delta\Omega$ and $\Delta\lambda$ approach 0 is the spectral radiance, L_λ, at the point (xyz) in the direction $(x'y'z') \rightarrow (xyz)$ for the wavelength λ. Symbolically

$$\lim_{\substack{\Delta A\to 0\\ \Delta\Omega\to 0\\ \Delta\lambda\to 0}} \frac{\Delta_\lambda[\Delta_{A'}(\Delta_A\Phi)]}{\Delta\lambda\,\Delta\Omega\,\Delta A\cos\theta} = L_\lambda(x\,y\,z\,\theta\,\phi\,\lambda) \qquad (1)$$

where $(\theta\phi)$ represent the polar and azmuthal angles of a spherical coordinate system whose origin is at (xyz) and polar axis is in the direction of the surface normal n. From calculus

$$L_\lambda = \frac{\partial^3\Phi}{\partial\lambda\,\partial\Omega\,\partial A\cos\theta} \qquad (2)$$

In addition, the radiant flux in a wavelength interval $\lambda_2 - \lambda_1$, propagating through an area A and solid angle Ω, whose apex is at A, is

$$\Phi = \int_{\lambda_1}^{\lambda_2}\int_{\Omega}\int_{A} L_\lambda\, dA\cos\theta\, d\Omega\, d\lambda \qquad (3)$$

The common unit for spectral radiance is watts (centimeters)$^{-2}$ (steradian)$^{-1}$ (centimeter)$^{-1}$.

Since spectral radiance is associated with a point and a direction, it can be said to be associated with an optical ray through this point and in this direction. One might guess that because of this association, it should be possible to prove some sort of invariance between a ray and the spectral radiance. Such an invariance can be proved (1). The result is that, excluding losses due to reflection, scattering or absorption, the ratio of the spectral radiance to the square of the index of refraction of the medium along a ray is constant. Moreover, these losses may be taken into account through the spectral transmittance or reflectance of the ray by the surface, medium or optical element responsible for the loss. This spectral transmittance or reflectance, defined as the ratio of the emerging spectral radiance to the incident spectral radiance, may often be determined once and used thereafter.

Fig. 2, showing a familiar tungsten strip being imaged by a simple lens,

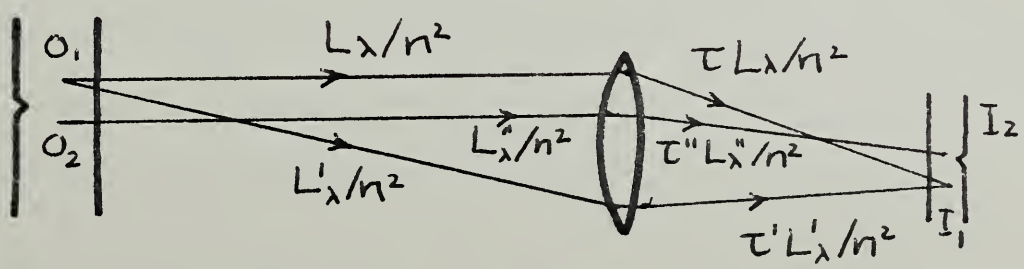

Fig. 2

illustrates this property of invariance. In this figure L_λ, L'_λ and L''_λ are the spectral radiances of the point O_1 and O_2, in the direction of the rays shown and $\tau_\lambda L_\lambda$, $\tau'_\lambda L'_\lambda$ and $\tau''_\lambda L''_\lambda$ are the spectral radiances of the image points I_1 and I_2 in the respective ray directions. The factors τ_λ, τ'_λ and τ''_λ are the spectral transmittances of the lens at the position and direction of the rays shown. Except for the transmittances, the radiance along a ray remains constant as long as the index of refraction does.

As indicated in Fig. 2 the spectral radiances associated with two rays from the same point, and of course from different points, on a source may be different. In general, the spectral radiance on a source is a function of both position and direction. However, to obtain the finite flux required for any actual measurements, a finite area and solid angle must be observed, and only the average radiance for this particular solid angle and area can be obtained. Moreover, as will be shown later, this average may be unusually weighted and a function of the particular spectroradiometer used. Thus care must be taken in describing the results of radiance measurements and such a commonly used phrase as the "spectral radiance of a source" should be avoided or at least accompanied with an explanation.

CALIBRATION EQUATION FOR A MONOCHROMATIC SOURCE

The basic radiometric calibration of any spectroradiometer involves the relationship between its electrical output and its radiant flux input, the latter usually expressed in terms of spectral radiance. In order to develop this relationship it is convenient to introduce the coordinate systems illustrated in Fig. 3.

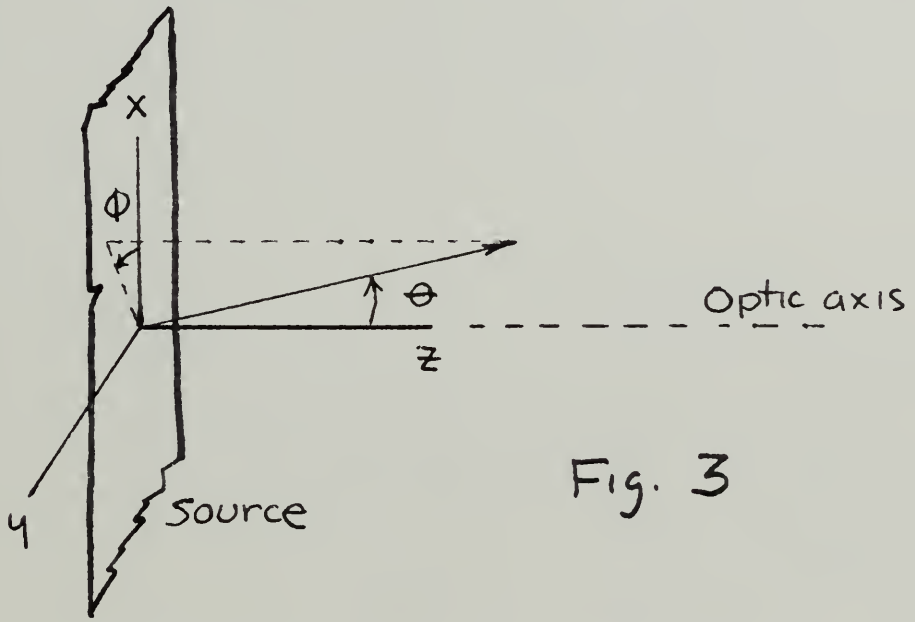

Fig. 3

A cartesian coordinate system is selected such that its origin is on the optic axis of the spectroradiometer and its (xy) plane is tangent to the source at this point. For simplicity we will assume the source is also a plane which is normal to the optic axis. Thus the z axis will coincide with the optic axis and a point on the radiating surface of the source can be represented by the coordinates (xy). At every point

(xy) on the source we consider another coordinate system, a spherical system with the polar axis parallel to the optic axis. The angle between any such polar axis (z axis) and the direction of the ray of interest is designated θ and the angle about the polar axis is called ϕ, as shown in Fig. 3. Using this coordinate system, the spectral radiance from an arbitrary point (xy) on the source and in an arbitrary direction ($\theta\phi$) can be denoted by the functional expression $L_\lambda = L_\lambda(xy\theta\phi)$. Fig. 4 is a schematic representation of a spectroradiometer. It includes

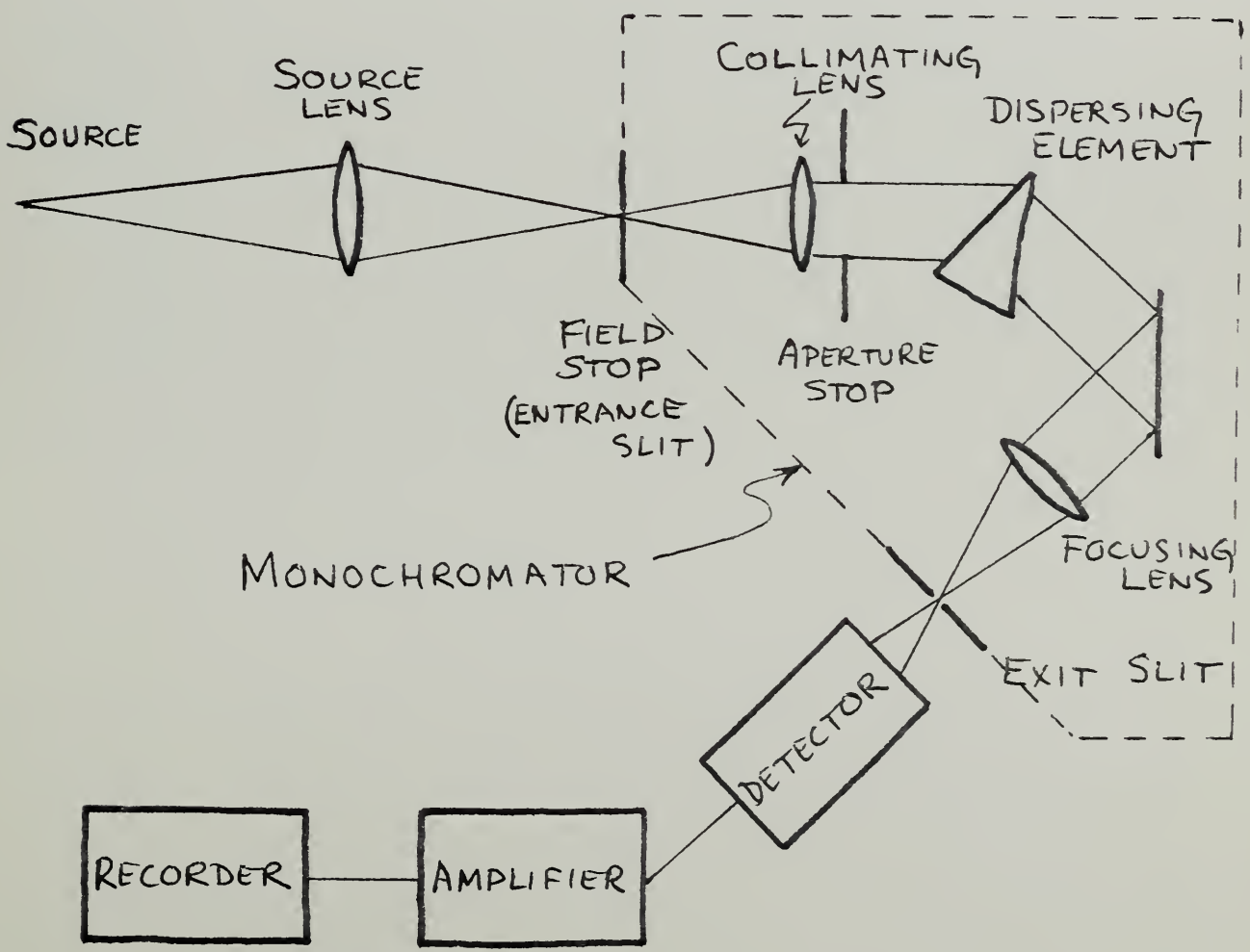

Fig. 4 SPECTRORADIOMETER

source optics, a monochromator, a detector, and required electronics and recorder or output meter. Let $L_\lambda(x_1 y_1 \theta_1 \phi_1)$ be the spectral radiance of the point $(x_1 y_1)$ on the source and in the direction $(\theta_1 \phi_1)$ corresponding to one of the rays in Fig. 4. Since the medium in which the optical elements are placed is the same throughout (usually air), the spectral radiance associated with this ray following the source lens is $L_\lambda(x_1 y_1 \theta_1 \phi_1)\ \tau'_\lambda(x_1 y_1 \theta_1 \phi_1)$ where $\tau'_\lambda(x_1 y_1 \theta_1 \phi_1)$ is the spectral transmittance of the source lens for this particular ray. The spectral radiance of the ray following the collimating lens is $L_\lambda(x_1 y_1 \theta_1 \phi_1)\ \tau'_\lambda(x_1 y_1 \theta_1 \phi_1)\ \tau''_\lambda(x_1 y_1 \theta_1 \phi_1)$ and continuing in this manner, $L_\lambda(x_1 y_1 \theta_1 \phi_1)\ \tau(x_1 y_1 \theta_1 \phi_1)$ is the spectral radiance of the ray falling on the detector where $\tau_\lambda(x_1 y_1 \theta_1 \phi_1)$ is the product of the individual transmittances of each of the optical components for this ray. In general $\tau_\lambda(xy\theta\phi)$ is the spectral transmittance of the entire spectroradiometer for the ray characterized by the coordinates $(xy\theta\phi)$ where (xy) is the point on the source where the ray originates and $(\theta\phi)$ is its initial direction.

The transmittance of an element may also depend on the polarization associated with the spectral radiance or ray in question. Since most sources of radiometric interest are either unpolarized or only slightly polarized, we will assume, at least for the present, that the flux incident on the spectroradiometer is unpolarized. Corrections for this

assumption not being valid will be considered in a later section.

If the source in Fig. 4 emits radiation at only one wavelength, λ_o, or more meaningfully emits radiation in a wavelength band, $\Delta\lambda$, which is very small compared to the spectral band passed by the spectroradiometer, the total radiant flux which is emitted by the source and which will enter the spectroradiometer is

$$\Phi_{in}(\lambda_o) = \Delta\lambda \iiiint L_\lambda(x\,y\,\theta\,\phi\,\lambda_o)\, dx\, dy \cos\theta \sin\theta\, d\theta\, d\phi \qquad (4)$$

where $\sin\theta d\theta d\phi$ is the differential solid angle $d\Omega$ and $dxdy$ is the dA of Eq. (3). The limits of integration for x and y are determined by the entrance window (2) or effective target area and for θ and ϕ by the solid angle subtended by the entrance pupil (2) which is determined by the aperture stop as indicated in Fig. 4. If the spectroradiometer is set on wavelength λ_o, the corresponding radiant power reaching the detector is

$$\Phi_{out}(\lambda_o) = \Delta\lambda \iiiint L_\lambda(x\,y\,\theta\,\phi\,\lambda_o)\, \tau_\lambda(x\,y\,\theta\,\phi\,\lambda_o)\, dx\, dy \cos\theta \sin\theta\, d\theta\, d\phi \qquad (5)$$

and the voltage output from the recorder is

$$V(\lambda_o) = \Delta\lambda\, G \iiiint L_\lambda(x\,y\,\theta\,\phi\,\lambda_o)\, \tau_\lambda(x\,y\,\theta\,\phi\,\lambda_o)\, R_\lambda(x\,y\,\theta\,\phi\,\lambda_o)\, dx\, dy \cos\theta \sin\theta\, d\theta\, d\phi \qquad (6)$$

where $\mathcal{R}_\lambda (xy\theta\phi\lambda_o)$ is the spectral response of the detector* for the ray characterized by the coordinates $(xy\theta\phi\lambda_o)$ and G* is the combined gain and response of the amplifier and recorder.

Eq. (6) is the calibration equation desired for a "monochromatic" source; that is, a source where the spectral radiance is constant within a small spectral band $\Delta\lambda$, defined above, and zero elsewhere. For a more general type source, the slit function concept is required as will be shown in the next section.

THE SLIT FUNCTION

If the source or beam of radiation that one is observing is not a narrow spectral line (monochromatic source), an integration relative to wavelength must be performed. The question arises as to what the limits of the wavelength integration should be. We shall try to answer this question by considering a few simple examples.

One of the most common conditions when using a spectroradiometer is that the entrance and exit slit widths are equal and the optical magnification of the entrance slit in the plane of the exit slit is one. Thus, the image of the entrance slit is the same size as the exit slit.

*For a photomultiplier tube, the units for $\mathcal{R}_\lambda$ are amperes per watt. In the present case the units for G are volts per ampere.

Let us assume that the entrance slit is irradiated by radiation for which the spectral radiance is constant with both wavelength and with position and direction of incidence on the entrance slit. Also, let us assume that the spectral transmittance of the monochromator is constant with respect to wavelength and that the spectroradiometer is set for a wavelength λo. The latter statement means that radiation of wavelength λo passing through an infinitesimal strip centered in the entrance slit and through the monochromator will fall on a similarly centered strip in the exit slit. Moreover, since the dispersion of the monochromator will generally vary negligibly over the width of the entrance or exit slit, all the rays corresponding to λo incident on the entrance slit and getting through the monochromator to the plane of the exit slit will fall on and pass through the exit slit. This assumes perfect (no aberrations) ray (no diffraction) imagery and is illustrated in Fig. 5a

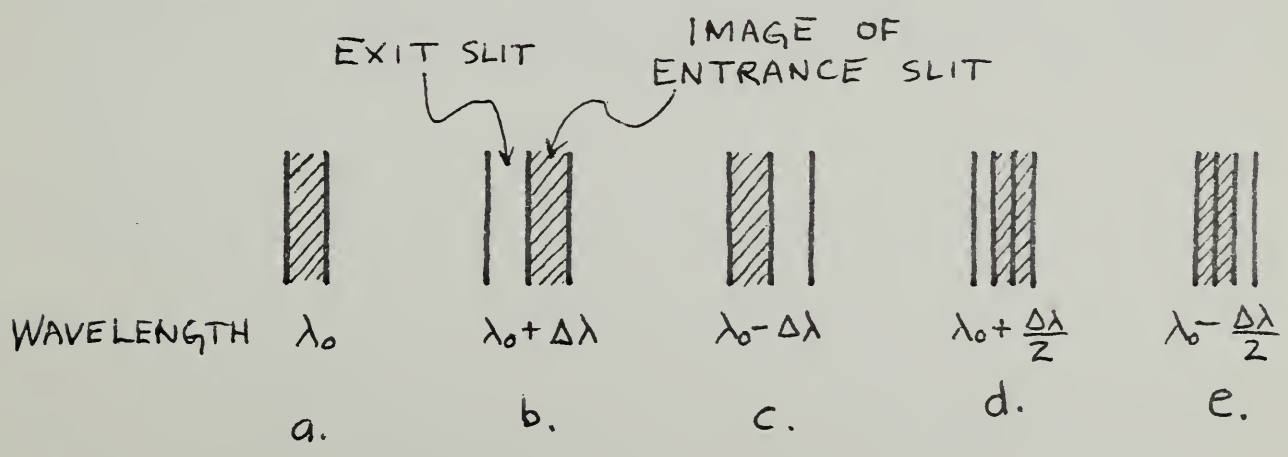

Fig. 5 POSITION OF IMAGE OF ENTRANCE SLIT AS A FUNCTION OF WAVELENGTH

where the image of the entrance slit produced by radiation of wavelength λo is superimposed on the exit slit. Images corresponding to other wavelengths will fall on either side of the λo image. Thus, there will be a wavelength, $\lambda o + \Delta\lambda$, such that its image will be sufficiently displaced to just miss getting through the exit slit (Fig. 5B). A similar situation occurs on the other side of the exit slit for $\lambda o - \Delta\lambda$. For wavelengths $\lambda o + \Delta\lambda/2$ and $\lambda o - \Delta\lambda/2$, half the image of the entrance slit will pass through the exit slit. Fig. 6 is a plot of the fraction of

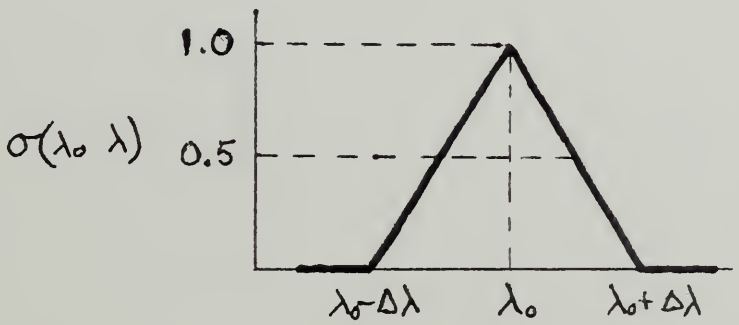

Fig. 6 IDEALIZED SLIT FUNCTION FOR EQUAL ENTRANCE AND EXIT SLITS

radiant flux of wavelength λ relative to that of wavelength λo which gets through the exit slit when the spectroradiometer is set on wavelength λo. Such a plot or function is called a slit or apparatus function and will be denoted by the symbol $\sigma(\lambda o\ \lambda)$.

For the simple ideal case described, the slit function is an isosceles triangle with its peak at λo and the width of its base equal

to $2\Delta\lambda$. The width at half-height, $\Delta\lambda$, sometimes referred to as the spectral slit width, is approximated by $\Delta S/(dx/d\lambda)$ where ΔS is the slit width and $dx/d\lambda$ is the linear dispersion of the monochromator. Fig. 7

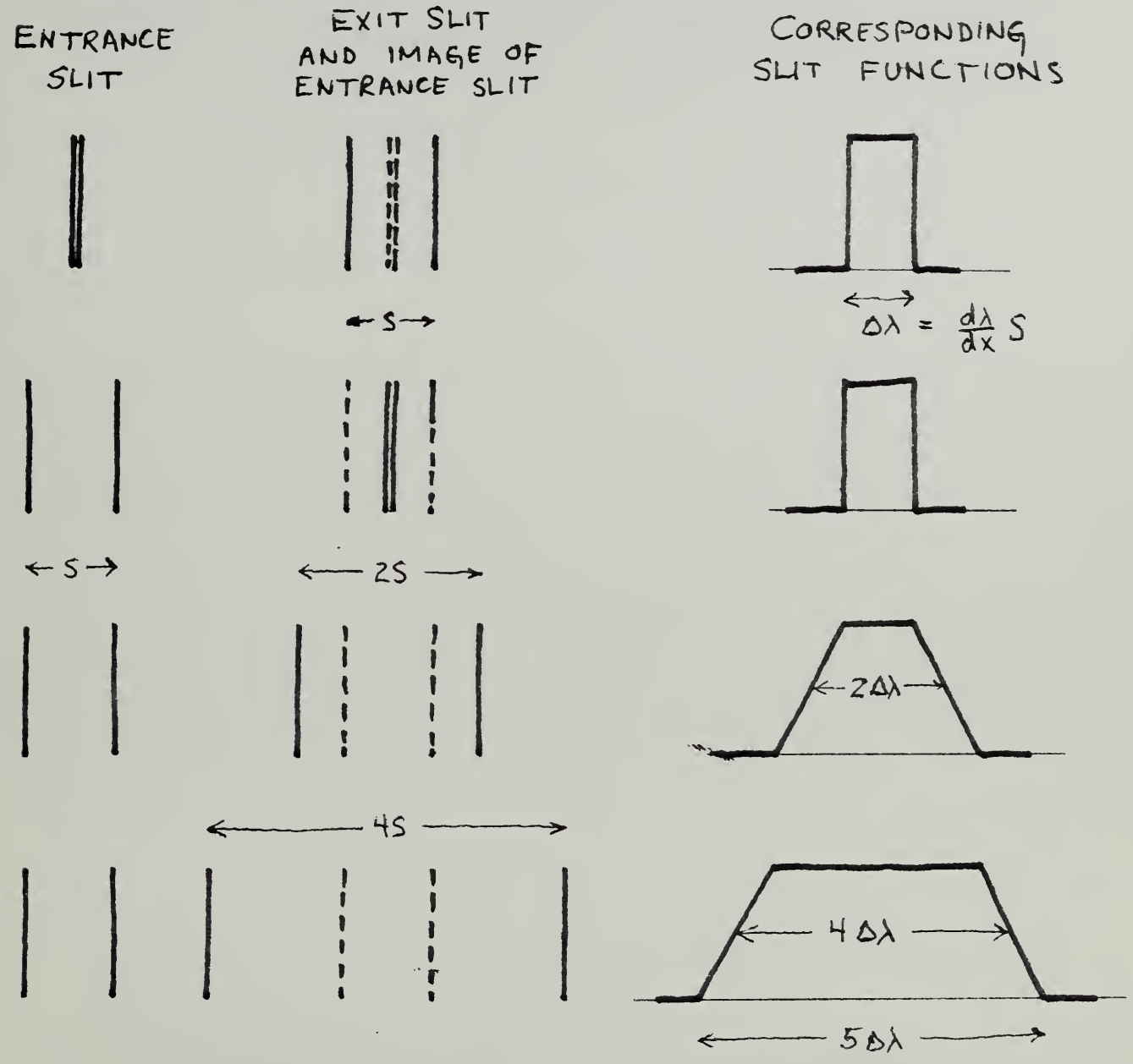

Fig 7 IDEALIZED SLIT FUNCTIONS FOR UNEQUAL ENTRANCE AND EXIT SLITS

shows the perfect ray slit functions for cases when the entrance and exit slit widths are not equal but at least one is large compared to $(\lambda o/w)f$. The slit functions are either rectangular or trapezoidal and their width at half-height is equal to the width of the wider of the two slits divided by the dispersion.

For the real case, where diffraction and possibly optical aberrations or even imperfect optical adjustment is present, the slit functions shown in Figs. 6 and 7 are only first approximations to the actual slit functions. The approximations may be quite good when at least one of the slits are wide compared to the distance between the peak and first minimum of the diffraction pattern associated with the image of the entrance slit in the plane of the exit slit. This distance is approximately equal to $(\lambda o/w)f$ where w is the diameter of the aperture stop and f is the focal length of the focusing lens in Fig. 4. Diffraction, aberrations, and imperfect optical adjustment will tend to broaden, round off the corners and extend the "wings" of the slit function as illustrated in Fig. 8.

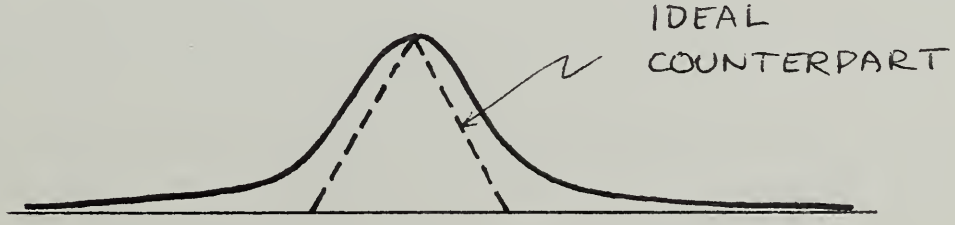

Fig. 8 TYPICAL REAL SLIT FUNCTION

In general, accurate slit functions must be obtained experimentally and a technique for doing this will be presented later.

GENERAL CALIBRATION EQUATION

From the definition of the slit function, the radiant flux reaching the detector in the spectroradiometer for an arbitrary spectral radiance input is obtained by including the slit function in the integrand of Eq. (5) and replacing $\Delta\lambda$ with an integration relative to wavelength. Denoting the slit function, when the spectroradiometer is set on λo by $\sigma(\lambda o\ \lambda)$, the output signal from the recorder for an arbitrary input is therefore given by

$$V(\lambda_o) = G\int\int\int\int\int\int L_\lambda(x\,y\,\theta\,\phi\,\lambda)\,T_\lambda(x\,y\,\theta\,\phi\,\lambda)\,R_\lambda(x\,y\,\theta\,\phi\,\lambda)\,\sigma(\lambda_o\,\lambda)\,dx\,dy\cos\theta\sin\theta\,d\theta\,d\phi\,d\lambda \qquad (7)$$

where the wavelength integration is over the wavelength range for which the integrand is non-zero. These limits of integration for a continuous source are usually determined by the extent of the slit function and for a spectral line source by either the slit function or the spectral line.

Eq. (7) emphasizes the many factors that can affect the output of the spectroradiometer. Fortunately the equation can be simplified significantly when the spectral radiance of all the rays incident on the spectroradiometer are independent of all variables except wavelength. For the most accurate radiometric measurements this is an important requirement, and for some sources is realized by viewing a small enough area and solid angle*. When this is not possible, an integrating sphere may be used and this will be discussed later in the section on Spectral Irradiance. In addition, a method for estimating the magnitude of the error when $L_\lambda(xy\theta\phi\lambda) \neq L_\lambda(\lambda)$ will be presented in the section on Higher Order Effects.

Assuming that L_λ is independent of (xy); i.e., a uniform target or source, and of $(\theta\phi)$; i.e., a lambertian source, Eq. (7) may be written

*Generally the radiance associated with rays from different points vary significantly more than that from the same point but a different direction. Thus, usually the field stop must be reduced but not the aperture stop. This can be confirmed by determining the radiance of the target as a function of $(xy\theta\phi)$ using a very small field and aperture stop.

$$V(\lambda_0) = G \int L_\lambda(\lambda)\, \sigma(\lambda_0 \lambda) \left[\iiiint \tau_\lambda(x y \theta \phi \lambda)\, \mathcal{R}_i(x y \theta \phi \lambda)\, dx\, dy \cos\theta \sin\theta\, d\theta\, d\phi \right] d\lambda \qquad (8)$$

$$V(\lambda_0) = G \int L_\lambda(\lambda)\, \sigma(\lambda_0 \lambda)\, \mathcal{R}_\lambda^e(\lambda)\, d\lambda \qquad (9)$$

where $\mathcal{R}_\lambda^e(\lambda)$ is the multiple integral in Eq. (8) and will be called the effective spectral response of the spectroradiometer. Thus, if $\mathcal{R}_\lambda^e(\lambda)$ can be determined experimentally, the equation relating the spectral radiance incident on the spectroradiometer to the output signal of the instrument can be simplified significantly. Fortunately it can, as will be shown in the next section. It should be emphasized, however, that Eq. (9) applies only to the above described idealized source and that $\mathcal{R}_\lambda^e(\lambda)$ changes if the field or aperture stop is modified. Also required in the derivation of the equation is the assumption that the effective spectral response does not depend on the magnitude of the flux incident on the detector and that the gain of the electronic system, G, is independent of the magnitude of the electrical input signal.

EXPERIMENTAL DETERMINATION OF THE SLIT FUNCTION AND THE EFFECTIVE SPECTRAL RESPONSE

For many calibration problems it is necessary to know the effective spectral response $\mathcal{R}_\lambda^e$ and the slit function $\sigma(\lambda_o\ \lambda)$ of the spectroradiometer. Therefore, this section will be devoted to the determination of these functions.

The effective spectral response $\mathcal{R}_\lambda^e(\lambda)$ in Eq. (9) can be obtained for a particular spectroradiometer by spectrally scanning a source whose relative spectral distribution is known and doesn't change significantly over the wavelength range of the slit function. A blackbody, tungsten strip lamp or the positive crater of a graphite arc are suitable for this purpose if the spectral slit width is a few angstroms or less. Under these conditions, Eq. (9) can be reduced to

$$V(\lambda_o) = G\, L_\lambda(\lambda_o)\, R_\lambda^e(\lambda_o) \int \sigma(\lambda_o\ \lambda)\, d\lambda \qquad (10)$$

and

$$R_\lambda^e(\lambda_o) = \frac{V(\lambda_o)}{G\, L_\lambda(\lambda_o) \int \sigma(\lambda_o\ \lambda)\, d\lambda} \qquad (11)$$

For determining $\mathcal{R}_\lambda^e$ it is usually adequate to assume $\int\sigma(\lambda_o\lambda)d\lambda = C\,\frac{d\lambda}{dx}(\lambda_o)$ where $\frac{d\lambda}{dx}(\lambda_o)$ is the linear dispersion of the monochromator at λ_o. Then

$$\mathcal{R}_\lambda^e(\lambda_o) = \frac{V(\lambda_o)}{C \mathcal{G} L_\lambda(\lambda_o) \frac{d\lambda}{dx}(\lambda_o)} \qquad (12)$$

Thus, by dividing, at each wavelength, the recorder output of the spectral scan, V(λo), by the product of the spectral radiance of the source and the dispersion of the monochromator at that wavelength, one obtains a function proportional to the effective spectral response. As will be seen later, only the relative value of $\mathcal{R}_\lambda^e(\lambda)$ is required. However, it is not uncommon over a wide spectral scan for the amplifier gain to require change, and such changes in G must also be taken into account.

In this treatment it is required that $\mathcal{R}_\lambda^e(\lambda)$ not depend on the magnitude of the radiant flux passing through the monochromator or striking the detector because $\mathcal{R}_\lambda^e(\lambda)$ will usually be determined using a different σ and G than when the spectroradiometer is calibrated. Fortunately the requirement can be experimentally checked by simply determining $\mathcal{R}_\lambda^e(\lambda)$ with a number of sources having significantly different radiances.

The slit function can be obtained, at least in principal, by setting the spectroradiometer at the wavelength for which the slit function is

desired and filling the field and aperture stops with the flux from a number of monochromator sources each having the same radiance but slightly different wavelengths, all however falling within the wavelength range of the slit function. The spectroradiometer output for each of these sources is proportional to the product of the effective response of the spectroradiometer at the wavelength of the source and the value of the slit function corresponding to the monochromator wavelength setting and for the wavelength of the source. Thus, dividing this output at each wavelength by the effective response for that wavelength makes it possible to map out the slit function. However, this straightforward approach is quite impractical because "monochromatic" sources satisfying the above requirements are rarely if ever available. In some situations, a second monochromator could be used as a source, but this would require an extensive amount of work.

Fortunately, the slit function can be obtained, and rather simply, by using one "monochromatic" source and a number of monochromator wavelength settings instead of a number of sources and one setting. That is, the slit function can be obtained by a wavelength scan of a spectral line which is very narrow compared to the spectral slit width. Actually the spectral scan is not the slit function but its mirror image, reflected about the wavelength of the source. Fig. 9 illustrates

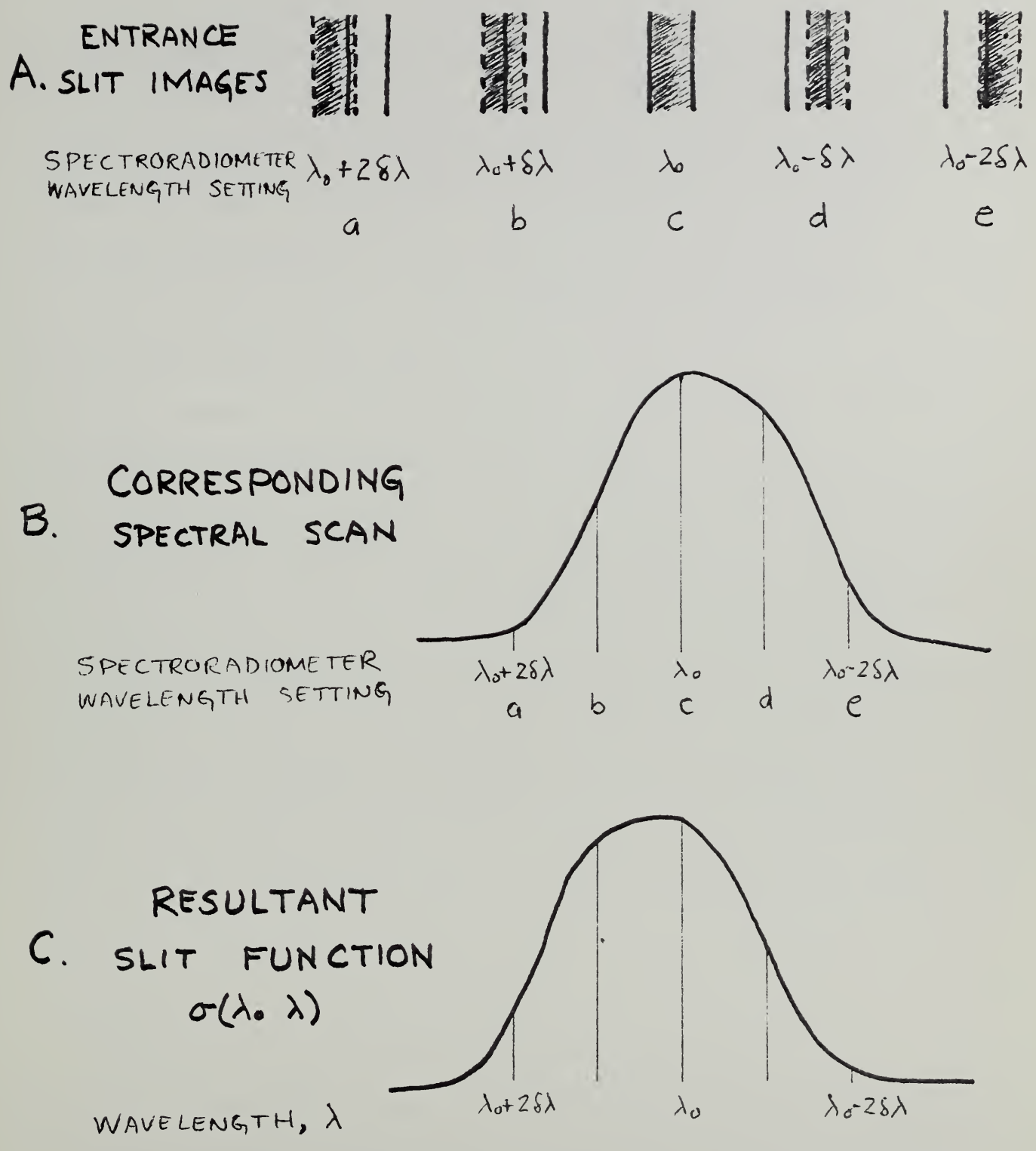

Fig. 9 RELATION BETWEEN SPECTRAL SCAN OF NARROW EMISSION LINE AND SLIT FUNCTION

why this is the case and why this method works. In Fig. 9A, the image of the entrance slit, which is irradiated with virtually monochromatic radiation, λo, is shown in the plane of the exit slit for various wavelength settings of the spectroradiometer. It should be noted that the irradiance of the images is not uniform, an effect that could be caused by improper optical adjustment of the spectrometer. Fig. 9B shows the recorder output for the spectral scan. Since the only wavelength present is λo, the value of the spectroradiometer effective response does not change significantly* and from the definition of the slit function, the recorder deflections are proportional to values of the slit function. However, except for the result at λo, the values do not correspond to the slit function for a monochromator setting λo. The deflection at "a" is proportional to $\sigma(\lambda o+2\delta\lambda \quad \lambda o)$ which is the value of the slit function for the wavelength λo when the monochromator is set at $\lambda o+2\delta\lambda$. Similarly the deflection at b is proportional to $\sigma(\lambda o+\delta\lambda \quad \lambda o)$, at c to $\sigma(\lambda o \quad \lambda o)$, at d to $\sigma(\lambda o-\delta\lambda \quad \lambda o)$ and at e to $\sigma(\lambda o-2\delta\lambda \quad \lambda o)$. Fortunately, the slit function usually changes negligibly over a wavelength interval corresponding to its own range. For

*Slight changes in $R_\lambda^e(\lambda)$ might be expected due to very small changes in the optical system resulting from the wavelength scan from $\lambda o+2\delta\lambda$ to $\lambda o-2\delta\lambda$.

example, the value of the slit function for a wavelength λo when the monochromator is set on $\lambda o+2\delta$ is equal to its value for a wavelength $\lambda o-2\delta$ when set on λo; that is, $\sigma(\lambda o+2\delta \;\; \lambda o) = \sigma(\lambda o \;\; \lambda o-2\delta)$. Similarly $\sigma(\lambda o+\delta \;\; \lambda o) = \sigma(\lambda o \;\; \lambda o-\delta)$, $\sigma(\lambda o-\delta \;\; \lambda o) = \sigma(\lambda o \;\; \lambda o+\delta)$ and $\sigma(\lambda o-2\delta \;\; \lambda o) = \sigma(\lambda o \;\; \lambda o+2\delta)$. Thus, the slit function $\sigma(\lambda o \;\; \lambda)$ is the mirror image shown in Fig. 9C of the spectral scan of the line with the plane of reflection being λo.

The above result can also be obtained directly from Eq. (9). Assume the monochromator is set at $\lambda o+x$. Since the narrow spectral line is at λo and the effective response and slit function is virtually constant over the extent of the line,

$$V(\lambda_o+x) = G\,R^e_\lambda(\lambda_o)\,\sigma(\lambda_o+x, \lambda_o) \int_{line} L_\lambda(\lambda)\,d\lambda \qquad (13)$$

As discussed in the previous paragraph

$$\sigma(\lambda_o+x \;\; \lambda_o) \simeq \sigma(\lambda_o \;\; \lambda_o-x) \qquad (14)$$

and

$$V(\lambda_o+x) = G\,R^e_\lambda(\lambda_o)\,\sigma(\lambda_o \;\; \lambda_o-x) \int_{line} L_\lambda(\lambda)\,d\lambda \qquad (15)$$

so that

$$\sigma(\lambda_o \; \lambda_o - x) = \frac{V(\lambda_o + x)}{G R_\lambda^e(\lambda_o) \int_{line} L(\lambda)\, d\lambda} \tag{16}$$

At the peak of the recorder trace, we have

$$V(\lambda_o) = G R_\lambda^e(\lambda_o)\, \sigma(\lambda_o \; \lambda_o) \int_{line} L(\lambda)\, d\lambda \tag{17}$$

and combining this with Eq. 16 results in

$$\sigma(\lambda_o \; \lambda_o - x) = \frac{V(\lambda_o + x)}{V(\lambda_o)}\, \sigma(\lambda_o \; \lambda_o) \tag{18}$$

But from our definition of the slit function $\sigma(\lambda o \; , \; \lambda o) \equiv 1$ and therefore

$$\sigma(\lambda_o \; \lambda_o - x) = \frac{V(\lambda_o + x)}{V(\lambda_o)} \tag{19}$$

SPECIFIC CALIBRATIONS

Spectroradiometers are usually calibrated by relating their output when observing an unknown source of spectral radiance to their output when observing a known or standard source of spectral radiance. The basic equations for such calibrations are obtained by applying Eq. (9) to both the standard and the unknown, i.e.

$$V^s(\lambda_0) = G^s \int L^s_\lambda(\lambda)\, \sigma(\lambda_0 \lambda)\, R^e_\lambda(\lambda)\, d\lambda$$
$$V(\lambda_0) = G \int L_\lambda(\lambda)\, \sigma(\lambda_0 \lambda)\, R^e_\lambda(\lambda)\, d\lambda \qquad (20)$$

where the superscript s refers to the standard. In this section, specific calibration equations for various types of spectral distributions will be derived and discussed.

a. Spectral radiance of a continuum

One of the most common type spectra of interest in radiometry is that which excludes spectral lines. Such a spectrum is usually obtained from the emission of solids and liquids and referred to as a continuum. The common standards of spectral radiance such as tungsten strip lamps or blackbodies have this type of spectrum.

The calibration equation for a continuum is very simple provided

the slit function or the effective spectral response of the spectro-radiometer is such that the spectral radiance functions in Eq. (20) may be taken outside the integral sign. Then

$$V^s(\lambda_o) = G^s L^s_\lambda(\lambda_o) \int \sigma(\lambda_o\, \lambda)\, R^e_\lambda(\lambda)\, d\lambda$$

$$V(\lambda_o) = G\, L_\lambda(\lambda_o) \int \sigma(\lambda_o\, \lambda)\, R^e_\lambda(\lambda)\, d\lambda \qquad (21)$$

and

$$L_\lambda(\lambda_o) = \frac{V(\lambda_o)\ G^s}{V^s(\lambda_o)\ G}\ L^s_\lambda(\lambda_o) \qquad (22)$$

This can be done when neither the standard nor the unknown spectral radiance changes significantly over the wavelength range for which the integrands in Eq. (21) are significant. In this case, it is not necessary to know the slit function or effective response of the spectro-radiometer. However, it is necessary to know that the above stated condition prevails which usually means the distant wings of the slit

function are negligible. This is usually the case for a double monochromator*. Incidentally, Eq. (22) assumes that the field stop and aperture stop is the same when viewing the unknown and standard. Otherwise, $\mathcal{R}_\lambda^e(\lambda)$, which is given by the multiple integral in Eq. (8) would not be the same for the two equations in Eq. (21). In addition, whenever possible the standard should be adjusted so that

$$\frac{V(\lambda_0)}{V^s(\lambda_0)} = \frac{G^s}{G} = 1 \qquad (23)$$

Then the accuracy of the measurement will not depend on the lack of linearity in the detector or amplifier.

If L_λ or L_λ^s can not be removed from the integral sign in Eq. (20), the calibration is considerably more difficult. Not only the slit function and the effective spectral response of the spectroradiometer are required but also the relative spectral distribution, $f(\lambda)$, of the

*A double monochromator is the name of the instrument in which two monochromators are used in series. The exit slit in Fig. 4 would then be the entrance slit of another monochromator.

unknown where

$$L_\lambda(\lambda) = C f(\lambda) \tag{24}$$

and C is a constant relative to wavelength. Fortunately, the relative spectral distribution $f(\lambda)$ need not be known as accurately as $L_\lambda(\lambda)$ is desired. The accuracy required will depend on the magnitude of $\sigma(\lambda_o \ \lambda)\ \mathcal{R}_\lambda^e(\lambda)$ at wavelengths distant from λo. This, of course, means that C may vary with wavelength and should be determined at each wavelength for which the spectral radiance is desired. Mathematically, if measurements with the spectroradiometer result in

$$V(\lambda_o) = K(\lambda_o)\ V^s(\lambda_o) \tag{25}$$

where K is the number relating the two outputs, then using Eq. (24) and Eq. (20)

$$C(\lambda_o) = \frac{K(\lambda_o) G^s \int L_\lambda^s(\lambda)\, \sigma(\lambda_o\, \lambda) R_\lambda^e(\lambda)\, d\lambda}{G \int f(\lambda)\, \sigma(\lambda_o\, \lambda)\, R_\lambda^e(\lambda)\, d\lambda} \tag{26}$$

which is the calibration equation for this case. If $f(\lambda)$ is not available, a zero order approximation, $f_0(\lambda)$, can be obtained by applying Eq. (22) as a function of wavelength and assuming the resulting $L_\lambda(\lambda)$

equals $f_0(\lambda)$. A first order approximation of $C(\lambda)$ obtained by using these $f_0(\lambda)$ in Eq. (26) can then be used for a first order approximation of $f(\lambda)$; that is, $f_1(\lambda) = C_1(\lambda)\, f_0(\lambda)$ which in turn can be used in Eq. (26) to obtain $C_2(\lambda)$. This is repeated until $C_{i+1}(\lambda) = C_i(\lambda)$ to well within the accuracy desired.

Eq. (26) rather than Eq. (22) may be required, even for moderate accuracies of about 5%, when using a single monochromator (rather than a double monochromator) in the situation when the spectral radiance functions of the standard and unknown are significantly different and when at least one of these functions has a very small value at the wavelength of interest relative to its value at other wavelengths. Fig. 10

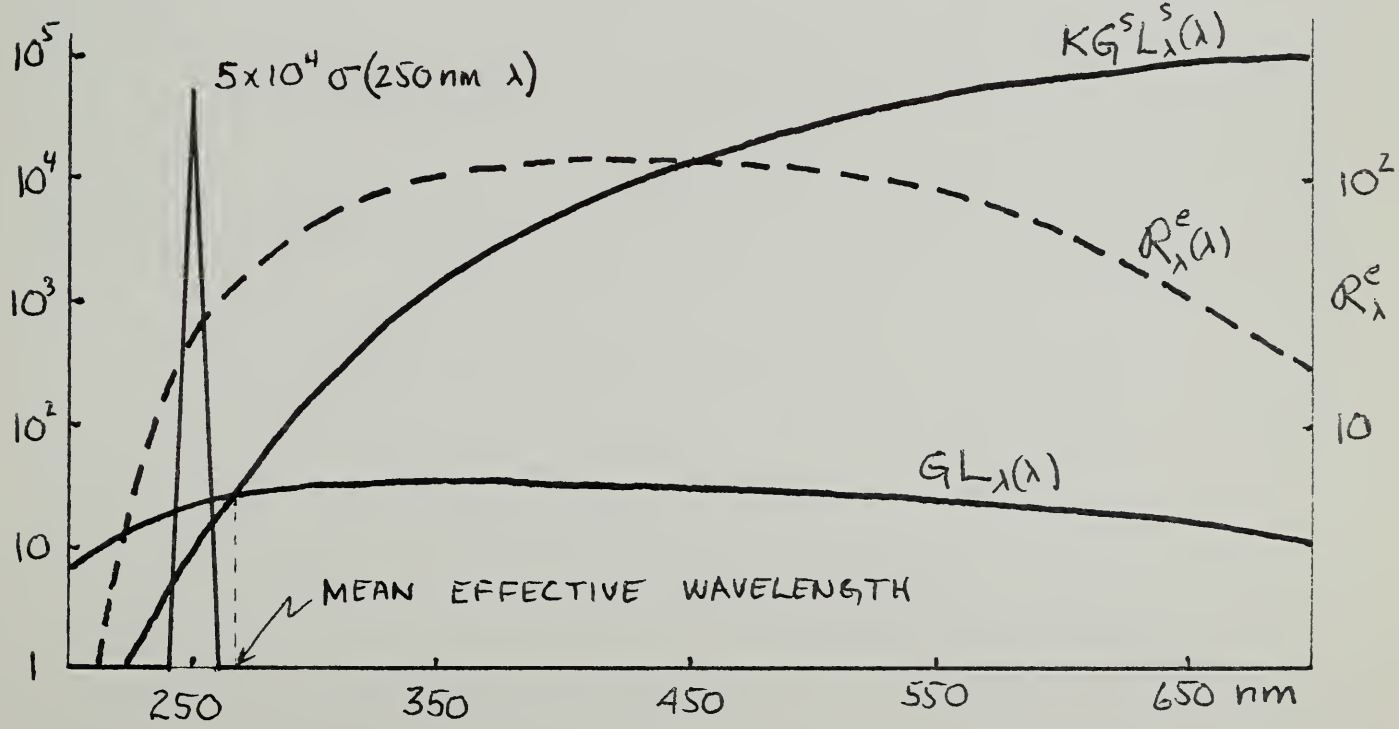

Fig 10

illustrates this problem for the case of the argon arc in Part II. It is assumed that the slit function has a constant value of 2×10^{-5} except for near 250 nm. As seen in the figure GL_λ (250 nm) differs from $KG^sL_\lambda{}^s$ (250 nm) by a factor of about two even though the simple calibration using Eq. (22) would indicate they are equal. The fact that $V(\lambda o) = K(\lambda o)\, V^s(\lambda o)$ or

$$G\int L_\lambda(\lambda)\,\sigma(\lambda_o\,\lambda)\,R^e_\lambda(\lambda)\,d\lambda = K(\lambda_o)G^s\int L^s_\lambda(\lambda)\,\sigma(\lambda_o\,\lambda)\,R^e_\lambda(\lambda)\,d\lambda \qquad (27)$$

merely means that $GL_\lambda = KG^sL^s{}_\lambda$ for at least one wavelength. This wavelength need not be λo. It can be obtained by combining its defining equation

$$G\,L_\lambda(\lambda') = K\,G^s L^s(\lambda') \qquad (28)$$

with Eq. (27), resulting in

$$\frac{\int L^s_\lambda(\lambda)\,\sigma(\lambda_o\,\lambda)\,R^e_\lambda(\lambda)\,d\lambda}{\int L_\lambda(\lambda)\,\sigma(\lambda_o\,\lambda)\,R^e_\lambda(\lambda)\,d\lambda} = \frac{L^s_\lambda(\lambda')}{L_\lambda(\lambda')} \qquad (29)$$

The wavelength λ' has had extensive use in optical pyrometry and is referred to as the mean effective wavelength (3) of the instrument for the two radiance functions.

In any serious work, even with a double monochromator, one should obtain estimates of $\sigma(\lambda o\ \lambda)\mathcal{R}_\lambda^e$ and $f(\lambda)$ and determine how well the effective wavelength, λ', agrees with the wavelength setting of the monochromator, λo. If the agreement isn't adequate, Eqs. (26) and (29) must be used or $\sigma(\lambda o\ \lambda)$ or $\mathcal{R}_\lambda^e$ improved by adding a filter or replacing the existing detector with one having a more appropriate response.

b. Intensity of a spectral line

When a spectrum of interest contains spectral emission lines, one is radiometrically concerned with either the spectral radiance at each wavelength of the line; that is, the shape of the line or the integral with respect to wavelength of the spectral radiance of the line. The latter is called the intensity of the line.

When determining the shape of a spectral line, the width of the slit function must be significantly less than the width of the line. Then the problem is equivalent to determining the spectral radiance of a continuum which has been presented. When the spectral slit width is approximately equal to the line width, determining the line shape or

width is very difficult, generally inaccurate, and essentially a research problem (4). It will not be considered in this report. When the spectral line is much narrower than the spectral slit width, the line intensity is usually all that can be determined. Fortunately, it is often all that is required.

Fig. 11 shows a typical spectral line, a standard continuous source,

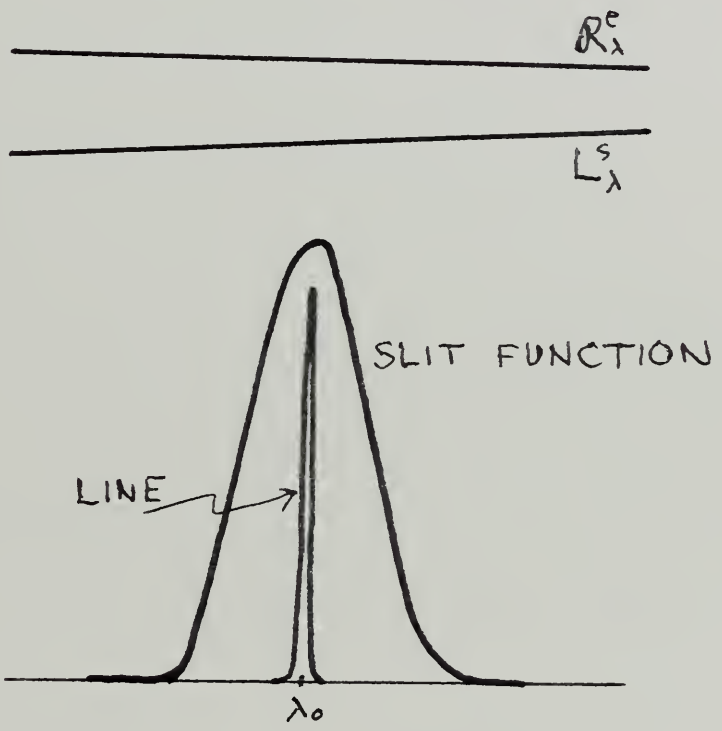

Fig. 11

effective response and slit function. Since L_λ^s and $\mathcal{R}_\lambda^e$ change negligibly

over the slit function and $\sigma(\lambda_o\ \lambda)$ changes negligibly over the line, Eq. (20) may be reduced to

$$V^s(\lambda_o) = G^s L^s_\lambda(\lambda_o) R^e_\lambda(\lambda_o) \int \sigma(\lambda_o\ \lambda)\, d\lambda$$

$$V(\lambda_o) = G\, \sigma(\lambda_o \lambda_o) R^e_\lambda(\lambda_o) \int_{line} L_\lambda(\lambda)\, d\lambda \qquad (30)$$

where $\int_{line} L_\lambda(\lambda)\, d\lambda$ is the line intensity.*

*In terms of atomic parameters

$$\int_{line} L_\lambda(\lambda) d\lambda = \frac{h \nu_{nm} A_{nm} N_n \Delta Z}{4\pi}$$

where h is the Planck constant, ν_{nm} the frequency of the line, A_{nm} its transitional probability, N_n the volume density of the emitter in the initial state of the transition and ΔZ the depth of the volume being observed.

Since $\sigma(\lambda o\ \lambda o) \equiv 1$, combining Eqs. (30)

$$\int_{line} L_\lambda(\lambda)\, d\lambda = \frac{V(\lambda_o)\, G^s}{V^s(\lambda_o)\, G} L^s_\lambda(\lambda_o) \int \sigma(\lambda_o\, \lambda)\, d\lambda \qquad (31)$$

Thus, in this measurement, the integral of the slit function, sometimes called the effective spectral slit width, $\Delta\lambda^e$, is required and must be obtained experimentally. Note that $V(\lambda o)$ and $V^s(\lambda o)$ are outputs corresponding to only one wavelength, λo, of the spectroradiometer. In the case of a line, $V(\lambda o)$ will correspond to the peak of the wavelength scan over the line.

Eq. (31) is the equation for determining the intensity of a line in the case when the spectral line is completely contained within the essentially constant portion of the slit function as shown in Fig. 11. This never really occurs and some correction is required for that part of the line outside this region. The correction will depend primarily on the shape of the line in the distant wings. If this shape is known, an estimate of the required correction can be obtained from the equation

$$\text{CORRECTION} = \frac{\int_{\lambda_o + \Delta\lambda^e/2}^{\infty} L_\lambda(\lambda)\, d\lambda}{\int_{\lambda_o}^{\infty} L_\lambda(\lambda)\, d\lambda} \qquad (32)$$

For a line with a shape proportional to $\frac{1}{(\lambda-\lambda o)^2 + \alpha^2}$ where α is the half-width (half the width of the line at its half radiance values) of the line, the correction is about 0.13 when the ratio of half the spectral slit width to line half width is 10 and about 0.01 when it is 100.

If it is not desirable to make the spectral slit width considerably greater than the line width, possibly because other spectral lines are too near the particular line of interest, Eq. (31) can not be used to obtain the line intensity. In this case, assuming the slit function is approximately the same width as the line, as illustrated in Fig. 12a,

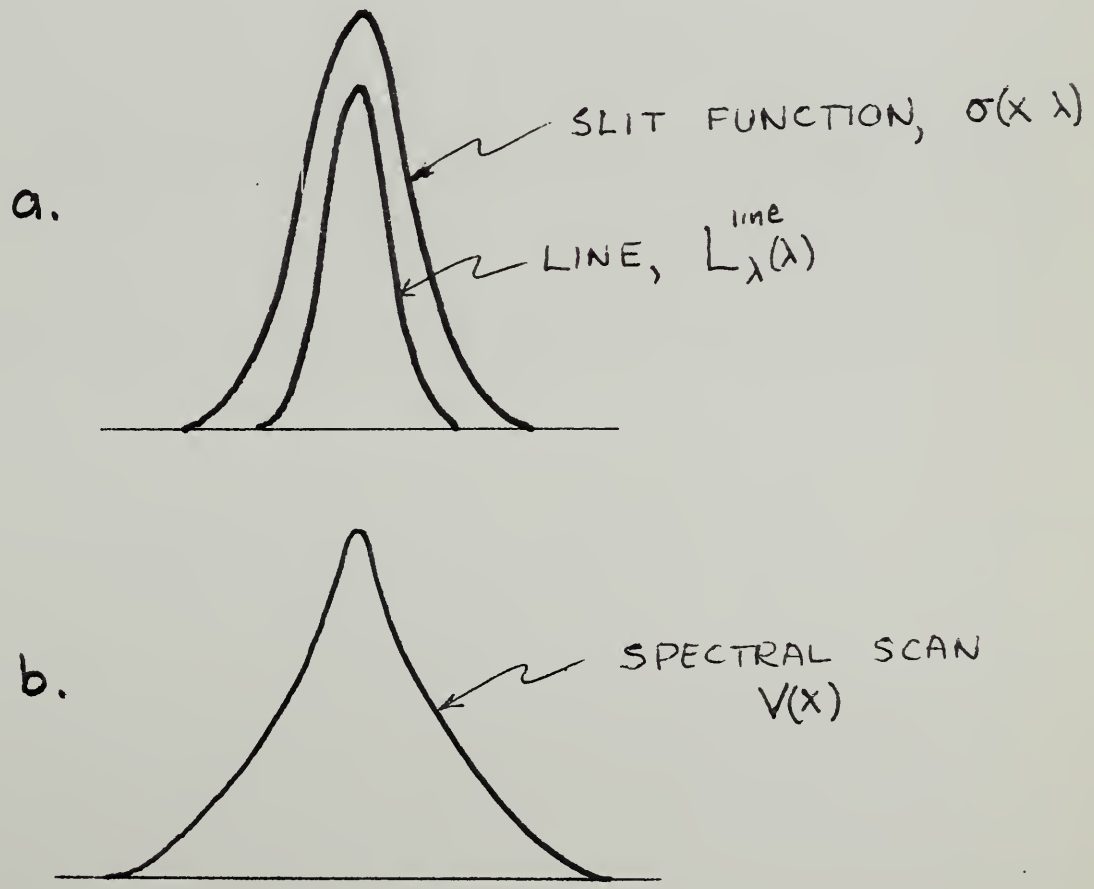

Fig. 12

Eq. (20) becomes

$$V^s(\lambda_o) = G^s L^s_\lambda(\lambda_o) R^e_\lambda(\lambda_o) \int \sigma(\lambda_o\ \lambda)\ d\lambda \qquad (31)$$

as before, but

$$V(\lambda_o) = G\, R^e_\lambda(\lambda_o) \int L_\lambda(\lambda)\, \sigma(\lambda_o\ \lambda)\, d\lambda \qquad (32)$$

Since we are now allowing λo to vary, let's call it x. V(x) is the spectroradiometer's spectral scan over the line and is shown in Fig. 12b. The integral of this scan; that is, the area under the curve in Fig. 12b is

$$\int V(x)\, dx = G \int_x R^e_\lambda(x) \left(\int_\lambda L_\lambda(\lambda)\ \sigma(x\ \lambda)\, d\lambda \right) dx \qquad (33)$$

Usually the effective response changes negligibly over the extent of such an integration. Therefore

$$\int V(x)\, dx = G\, R^e_\lambda(\lambda_o) \int_x \int_\lambda L_\lambda(\lambda)\, \sigma(x\ \lambda)\, d\lambda\, dx \qquad (34)$$

Interchanging the order of integration

$$\int V(x)\,dx = G\,R^{e}_{\lambda}(\lambda_o) \int L_{\lambda}(\lambda) \left(\int_{x} \sigma(x\ \lambda)\,dx \right) d\lambda \qquad (35)$$

Since the slit function is really a function of the difference of its two variables, integration relative to either of its two variables results in the same value, i.e., the area under the slit function. Moreover, if the slit function does not change over the full extent of the line, its area will not change and can be removed from within the line integration. Thus

$$\int V(x)\,dx = G\,R^{e}_{\lambda}(\lambda_o) \left(\int_{x} \sigma(x\ \lambda)\,dx \right) \left(\int_{\lambda} L_{\lambda}(\lambda)\,d\lambda \right) \qquad (36)$$

and using the above stated fact that $\int\sigma(x\ \lambda)dx = \int\sigma(x\ \lambda)d\lambda$ and Eq. (31)

$$\int L(\lambda)\,d\lambda = \frac{G^{s} \int V(x)\,dx}{G\,V^{s}(\lambda_o)}\ L^{s}_{\lambda}(\lambda_o) \qquad (37)$$

If one is concerned with the error associated with the variation

of $L_\lambda^s(\lambda)$ over the wavelength range of integration, consider the situation where the standard is a 2500 K blackbody. For this source, the spectral radiance varies for a wavelength interval of one angstrom by about 0.01% at 10 000 A and about 0.5% at 2500 A. As before, a correction must be applied for not integrating the recorder trace over the distant wings of the line.

c. Intensity of several spectral lines

It is not uncommon to have a spectrum in which there are a number of spectral lines within the spectral slit width as shown in Fig. 13.

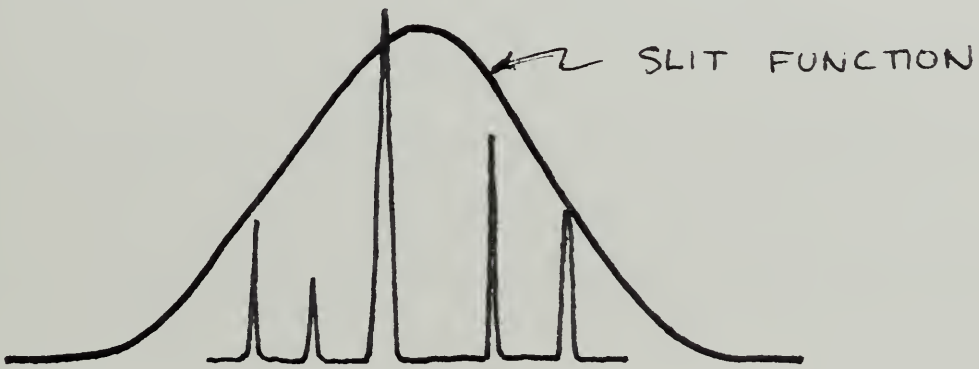

Fig. 13

These lines will not be seen individually and all one can determine is the total intensity of all the lines. With the slit function shown in Fig. 13 it is necessary to integrate the recorder trace and use Eq. (37).

The numerical integration involved can be avoided by using the rectangular slit function (one slit much wider than the other) shown in Fig. 14.

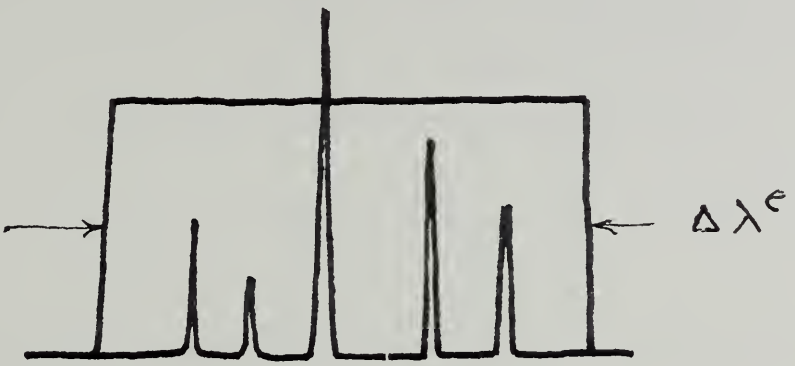

Fig. 14

Then the total intensity of the lines can be obtained from Eq. (31).

d. Combination of a continuum and a spectral line

This is a common occurrence when hot emitting gases are surrounding a solid (positive crater of a graphite arc) or when a gas is sufficiently hot to ionize some of the atoms (electrons and ions in a plasma emit a continuum while the atoms and ions also emit lines). In applying Eq. (20) to a single line and continuum as shown in Fig. 15

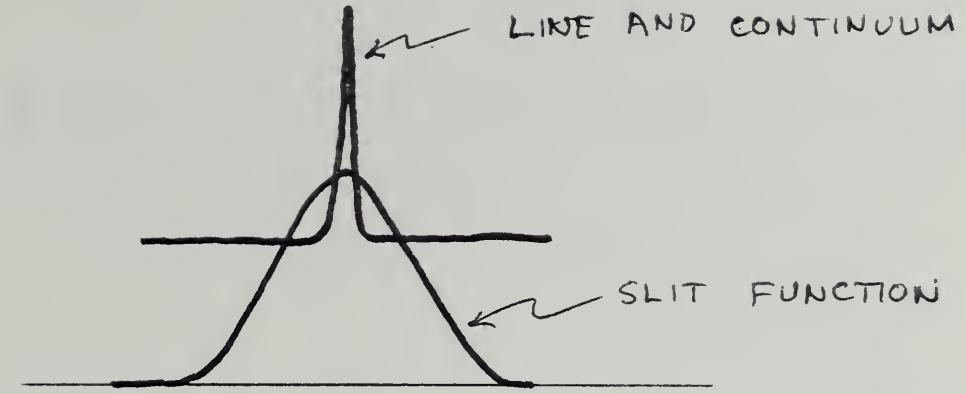

Fig. 15

one can express the unknown spectral radiance as the sum of line and continuum radiances resulting in

$$V(\lambda_0) = G R^e_\lambda(\lambda_0)\left[\int_{line} L^{line}_\lambda(\lambda)\,d\lambda + L^{cont.}_\lambda(\lambda_0)\int \sigma\, d\lambda\right] \qquad (38)$$

Using the first of Eqs. (30), one obtains

$$\frac{1}{\Delta\lambda^e}\int L^{line}_\lambda\, d\lambda + L^{cont.}_\lambda(\lambda_0) = \frac{V(\lambda_0)\,G^s}{V^s(\lambda_0)\,G} L^s_\lambda(\lambda_0) \qquad (39)$$

Thus in this situation one can obtain the sum of the continuum radiance plus the line intensity averaged over the effective spectral slit width. Relative to the continuum, as before, this implies the distant wings of the slit function are negligible and don't contribute to the output.

The extension to several lines plus a continuum can be made in the same manner as was done for several lines alone.

STANDARDS OF SPECTRAL RADIANCE

The most common standard of spectral radiance is the tungsten strip lamp. The gas filled version of this lamp can be used at blackbody temperatures varying from about 2400 K at 2500 nm to 2900 K at 210 nm. A typical strip is 3 mm × 40 mm and has uniformity of 1% over a central area of about 0.5 mm by 1.0 mm. Currents varying from 18 to 45 amps with voltages up to 13 volts depending on the model lamp are required. A current uncertainty of .1% corresponds to about .4% uncertainty in spectral radiance at 650 nm and this varies roughly inversely with wavelength (i.e., .8% uncertainty at 325 nm). Various models of the lamps are available from General Electric, Inc. in the United States and General Electric Limited in England. The lamps may be calibrated using an optical pyrometer and published emissivities* (5,6). The detailed procedure has been described in the literature (3). Calibrated lamps may be obtained from commercial laboratories or from the National Bureau of Standards. The estimated or reported uncertainties of these

*In our experience Larrabee's emissivities are preferred from 650 nm to 300 nm and Devos' from 650 nm to 850 nm.

calibrations, the wavelength range available and the approximate cost as of 1968 are given in Table 1.

Table 1

Source of Calibration	Uncertainty (%)						Approximate Cost
	2500 nm	850	650	300	250	210	
Pyrometer Calibration		5	2	7			Cost of lamp, provided calibrated pyrometer available
Commercial	3	4	4	7	8		$450
NBS		1	1	2	2	4	$1500

Another very useful standard of spectral radiance is the positive crater of a low current graphite arc (7). The spectral radiance of this source is similar to that of a 3800 K blackbody for a wide range of wavelengths in the visible and ultraviolet. In some wavelength regions there are very strong emission lines or bands from the arc column and below about 280 nm the arc column also contributes significantly to the continuum. The arc has been calibrated and used with an uncertainty (95% confidence) ranging from about 3% at 850 nm to 9% at 210 nm. It has a uniformity of about 1% over a diameter of about one millimeter.

This arc, developed specifically as a radiometric source, is commercially available from the Mole Richardson Co., Hollywood, California, for about $1500 and $3000, without and with a power supply, respectively. The major advantages of the graphite arc are its high radiance and the fact that it does not require a calibration. Its radiance corresponds to approximately the sublimation temperature of graphite. The disadvantages of the arc are that it cannot be used in a number of wavelength regions because of line emission, and it is less convenient to use than a strip lamp.

There are other sources that can be used as standards of spectral radiance, but, at present, either less is known about them, or they are not available commercially. Cavity radiators would be very useful standards provided their blackbody quality were confirmed and an accurate means of determining their temperature available. High temperature blackbodies are available commercially from a number of firms and, if sufficiently stable, could be calibrated at NBS. To date, no requests of this type have been received. The high pressure argon arc described in Part II of this report is also a very useful standard of spectral radiance between 200 nm and 300 nm but it is not currently available commercially. For details about this source one is referred to Part II.

Relative to the future, NBS is currently trying to improve and

extend infrared calibrations and standards. An improvement at 2500 nm to about 1% and an extension to 15 μm is contemplated within a year.

HIGHER ORDER EFFECTS

The general calibration equation, Eq. (9), requires that the spectral radiance, L_λ, be independent of $(xy\theta\phi)$ over the entrance window and pupil of the spectroradiometer. In addition, the optical radiation was represented by optical rays, assumed unpolarized, and the optical components considered perfect; thereby ignoring diffraction, polarization effects, and scattering and aberrations. The magnitude of the errors resulting from these assumptions and the methods of correcting these errors, if significant, will be presented in this section.

a. Lack of uniformity in spectral radiance, transmittance and response

If the transmittance of the spectroradiometer and response of the detector were uniform; i.e., constant for all rays passing through the instrument, no error would result from the spectral radiance being non-uniform. In this case, the new calibration equation obtained from Eq. (7) would be

$$V(\lambda_0) = G A \Omega \int \bar{L}_\lambda(\lambda)\, \tau(\lambda)\, R(\lambda)\, \sigma(\lambda_0, \lambda)\, d\lambda \qquad (40)$$

where

$$\overline{L}_\lambda(\lambda) = \frac{\iiiint L_\lambda(x\,y\,\theta\,\phi\,\lambda)\,dx\,dy\cos\theta\sin\theta\,d\theta\,d\phi}{A\Omega} \qquad (4$$

and

$$A\Omega = \underset{\text{entrance window \& pupil}}{\iiiint} dx\,dy\cos\theta\sin\theta\,d\theta\,d\phi \qquad (42)$$

$\bar{L}$ is the average radiance passing through the spectroradiometer as defined by Eq. (41). Thus, even if the source is non-uniform, the average radiance can be obtained using the previous treatment if τ and $\mathcal{R}$ are uniform.

In order to estimate the error committed when using Eq. (9) or Eq. (40) when τ and $\mathcal{R}$ are not uniform for all rays of interest, experimental measurements of the non-uniformities in L, τ and $\mathcal{R}$ are required. Using a very small target area, say 0.2 mm × 0.2 mm, and precisely translating the unknown source and standard in the x and y directions, it is possible to map the spectral radiance variations of the sources. An adequate angular mapping can be obtained with a larger target area, say 1 mm × 1 mm, but with an f/100 relative aperture. Typical maximum variations for the tungsten strip lamps, referred to in the Standard Sources section, are about 1% per millimeter and 1% per 6 degrees of

rotation. The variation in $\tau\mathcal{R}$ can be obtained by observing the output as a function of position of a small (say f/100) aperture stop placed in front of the source lens in Fig. 4. Typical variations of $\tau\mathcal{R}$ are 10 to 20% but can be greater for some monochromators and detectors. Thus, the maximum error $[\Delta L_\lambda \times \Delta(\tau_\lambda \mathcal{R}_\lambda)]$ caused by the non-uniformities assumed here in L_λ, τ_λ and $\mathcal{R}_\lambda$ is about .2% for a one millimeter target and an f/10 (about 6 degrees entrance angle) relative aperture. The actual error should be less than this maximum figure. Nevertheless, in any serious effort, the variations for the particular source and spectro-radiometer should be checked.

If the error is larger than desired, it can be decreased by various means. If the error is due largely to the (xy) non-uniformity in the target, a smaller target can be viewed, the detector more properly positioned as shown in Fig. 16a, or a field lens used as illustrated in Fig. 16b.

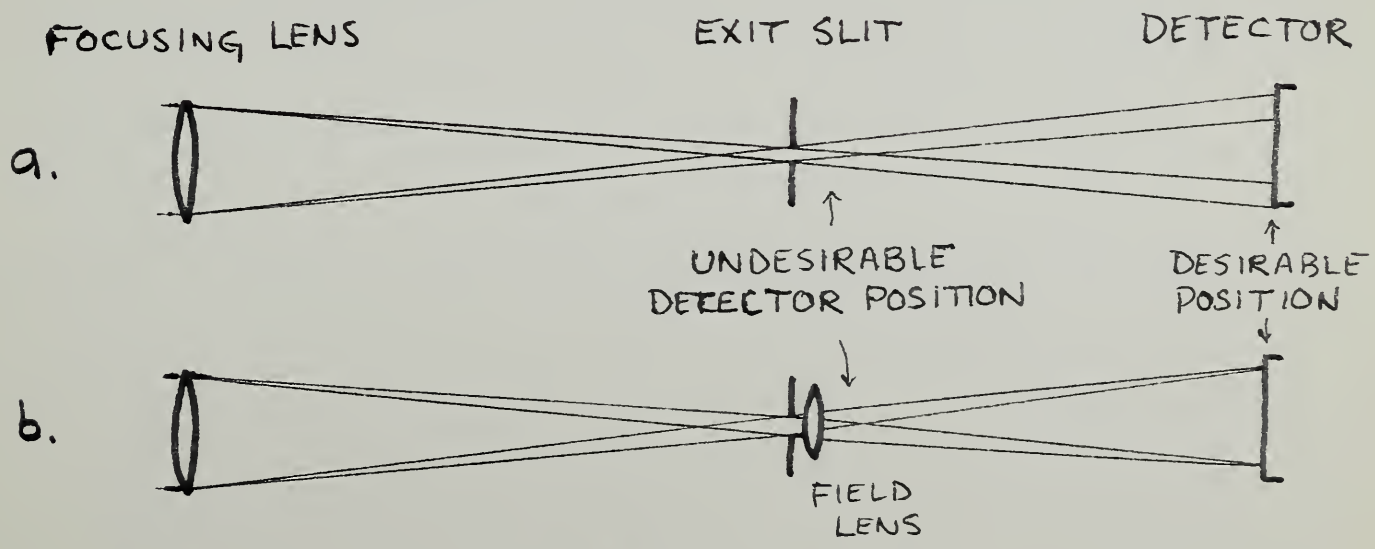

Fig. 16

The latter two approaches are designed so that each point of the target irradiates a large and similar detector area. If the error is due to large angular variations either in L_λ or $\tau_\lambda \rho_\lambda$, it can be reduced by decreasing the size of the aperture stop. These techniques are usually adequate. If not, an integrating sphere should be used, and its use will be discussed in the next section on Irradiance.

b. Size-of-source effect

The effects of scattering, diffraction and aberrations inside the monochromator are taken into account by the slit function. However, this is not the case for the source lens or any other optical elements located ahead of the entrance slit. If the unknown and standard source are identical in size, shape and non-uniformity, the effect of the above factors on the output will be the same for both sources and cancel in the comparison. Moreover, if the pre-monochromator optical system is well designed and the optics of high quality, diffraction and aberration effects will contribute less than 0.05% to this error (8) even when significantly different sized sources are being compared. For the standard sources referred to in this report, this can be realized if the optical system produces images in which a resolution of about 0.1 mm exists. Therefore, scattering is usually the major factor in this effect.

The kind of scattering being referred to is illustrated in Fig. 17.

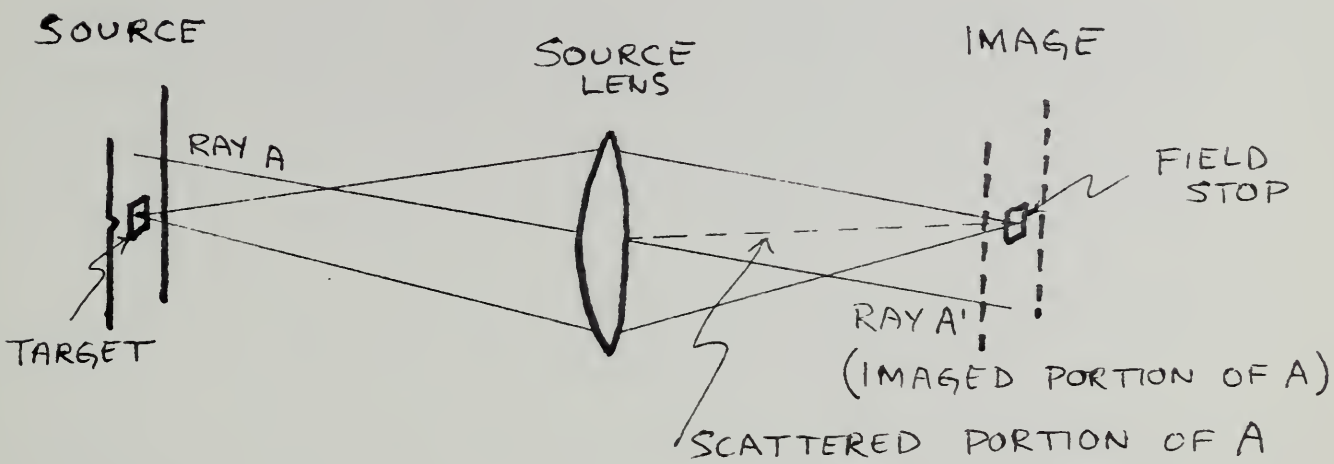

Fig. 17

In the figure, ray A would normally follow the path A' and not enter the field stop or entrance slit. However, a portion of the radiance associated with A is scattered into the monochromator. The amount scattered into the monochromator will depend on the size of the source and the condition of the optical element in question. We refer to it as a size-of-source effect. The result of this type scattering is that the larger of two sources will appear to have a greater radiance even if the radiances of the two target areas are the same. Typical increases vary, depending on the optical element, from 0.05% to 0.5%.

The size-of-source effect can be determined and corrected through

the use of a scattering function (9), a concept similar to that associated with the slit function. However, a more direct and simpler approach (8) is often adequate in radiometry. This involves observing an irradiated diffuse reflector containing a hole slightly larger than the target area. The hole, which emits no radiation, is imaged on the field stop. The only radiation entering the system is that scattered. By placing flock paper cut-outs simulating the size and shape of the standard and unknown sources on the diffuse reflector, the difference in the scattering for the two sources can be obtained. Corrections of this type have been made (8) with an estimated uncertainty of a few hundredths of a percent of the spectral radiance to be determined.

c. Polarization effect

Most spectroradiometers act as polarizers, or put in a different manner, have a transmittance which is a function of the polarization of an incident beam. The polarization in spectroradiometers varies with wavelength and has been observed, when the instrument incorporates a prism-grating double monochromator, to be as large as 0.2, where polarization is defined as $P = \left(\frac{Vmax - Vmin}{Vmax + Vmin}\right)$. Vmax and Vmin refers to the maximum and minimum outputs of the spectroradiometer relative to the direction of polarization of a linearly polarized flux incident on the instrument. Such a spectroradiometer polarization will result,

as will be shown below, in an error of 0.4% when an unknown source, linearly polarized to only 2% is compared to an unpolarized standard.

A complete experimental investigation of this effect; that is, determining the polarization properties of the spectroradiometer and the polarization of the source for arbitrary types of polarization is quite tedious and requires a quarter wave plate as well as a polarizer for each wavelength of interest (10,11). Fortunately, strip lamp sources and the prism and grating monochromators used by the author could be characterized as a combination of linearly polarized and unpolarized radiation, and therefore analyzed with only a polarizer.

The following method has been successfully used to accurately correct for the polarization effect for sources and spectroradiometers used by the author. The polarization of the unknown source is determined by observing it at a wavelength for which the spectroradiometer is unpolarized. If such a wavelength doesn't exist it can be realized by mounting and properly orienting two or three plane parallel plates of CaF_2, or other optical material transmitting over the wavelength range of interest, just beyond the exit slit of the monochromator. When the spectroradiometer is unpolarized, a linear polarizer placed normal to the optic axis and between a blackbody and the entrance slit will not affect the spectroradiometer output as the polarizer is rotated about

the optic axis. The polarizer and blackbody can then be used in the same manner at other wavelengths to determine the polarization of the spectroradiometer as a function of wavelength. In addition, the spectroradiometer can be used at its unpolarized wavelength, with the polarizer to determine the polarization of the unknown source. In each case, if the output varies with angle of rotation of the polarizer as $Vo + Vp \cos^2\theta$ the polarization is equivalent to an unpolarized component, Vo, and a linearly polarized component, Vp. When this is the case, one can use the simple vector representation and the calculations indicated in Table 2 on page 54 to correct for the polarization effect. In the example used in Table 2, the unknown would be corrected by increasing its spectral radiance by 0.4%.

d. Detector non-linearity and fatigue

In general, the response of detectors may vary with the magnitude of the radiant flux incident on them. Errors caused by this effect can be avoided if the standard is adjusted so that its monochromator output is equal to that for the unknown source. When this is not possible, the response of the detector should be experimentally determined as a function of the incident flux. This can be accomplished with a standard source whose radiance (and therefore the flux incident on the detector) can be varied in a known manner. Such a test will also require checking the response of the electronic system as a function

Table 2

	Relative Effective Response of Spectroradiometer	Spectral Radiance of Sources
Unpolarized	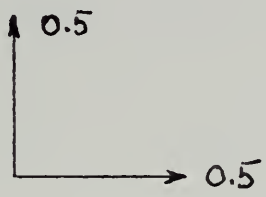	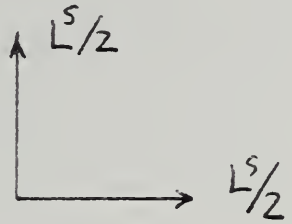
Polarized	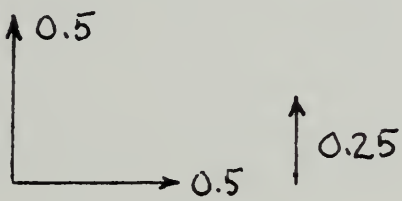	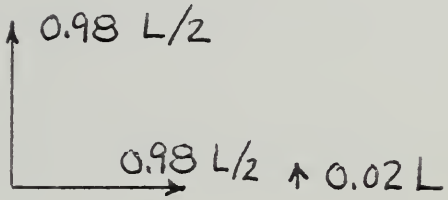

Assuming $V = KL^e$ and $V^s = KL^{s\,e}$ and using the unpolarized spectroradiometer to determine the L required in order for $V = V^s$

$$.5\,\frac{L^s}{2} + .5\,\frac{L^s}{2} = .5\left(.98\,\frac{L}{2} + .02L\right) + (.5)(.98)\,\frac{L}{2}$$

$$L = L^s$$

Similarly with the polarized spectroradiometer

$$(.5+.25)\left(.98\,\frac{L}{2} + .02L\right) + (.5)\left(.98\,\frac{L}{2}\right) = (.5+.25)\,\frac{L^s}{2} + .5\,\frac{L^s}{2}$$

$$L = .996\,L^s$$

Thus the spectral radiance determined with the polarized is found to be 0.4% less.

of its input signal.

The response of a detector may also change with the time a constant radiant flux is incident on it. In photomultipliers this effect is referred to as fatigue and depends on the magnitude of the incident flux, the anode current and the history of its exposure to radiant flux just prior to the time of interest. The lower the flux and anode current and the longer the period of irradiation, the smaller the fatigue rate. In tubes having an S20 type relative response, a fatigue rate of 0.01% per minute for an anode current of 10^{-8} amperes following a 30 minute irradiance with a flux of 10^{-10} watts is not uncommon. However, tubes characterized with such low fatigue rates, often changed differently on darkening for a minute or two following the 30 minute exposure. The response of some tubes changed by less than 0.02% while others changed (usually increased) by a few tenths of a percent. For larger fluxes and anode currents and shorter irradiation times, response changes of a few percent have been observed. Thus, the characteristics of each individual tube (or detector) should be investigated under the particular conditions and variables with which it will be used.

SPECTRAL IRRADIANCE

In previous sections of this report, the concept of spectral radiance and methods for determining it were developed. In this final section, another useful radiation parameter, spectral irradiance, will be introduced

and methods of measuring it presented.

a. Definition of spectral irradiance

Spectral irradiance, denoted by E_λ, is the radiant flux falling on a surface per unit area of the surface and per unit wavelength interval. More exactly, it is the limit of the ratio of the flux falling on a surface to the product of the area of the surface and the wavelength interval of the flux as the area and the wavelength interval are made to approach zero, i.e.,

$$E_\lambda(xyz\lambda) = \lim_{\substack{\Delta A \to 0 \\ \Delta\lambda \to 0}} \frac{\Delta_\lambda(\Delta_A \Phi)}{\Delta\lambda\, \Delta A} = \frac{\partial^2 \Phi}{\partial\lambda\, \partial A} \qquad (43)$$

where $\Delta_A\Phi$ represents the flux incident on an area ΔA surrounding the point (xyz) and $\Delta_\lambda(\Delta_A\Phi)$ is that portion of this flux in the wavelength interval $\Delta\lambda$ surrounding the wavelength λ. From the definitions of spectral radiance and spectral irradiance (Eqs. (2) and (43) respectively), these two parameters are related by the equation

$$E_\lambda(xyz\lambda) = \iint_{\text{solid angle } \Omega} L_\lambda(xyz\theta\phi\lambda)\cos\theta \sin\theta\, d\theta\, d\phi \qquad (44)$$

where $L_\lambda(xyz\theta\phi\lambda)$ is the spectral radiance at a point (xyz) and in a direction $(\theta\phi)$ and $E_\lambda(xyz\lambda)$ is the spectral irradiance at that same point.

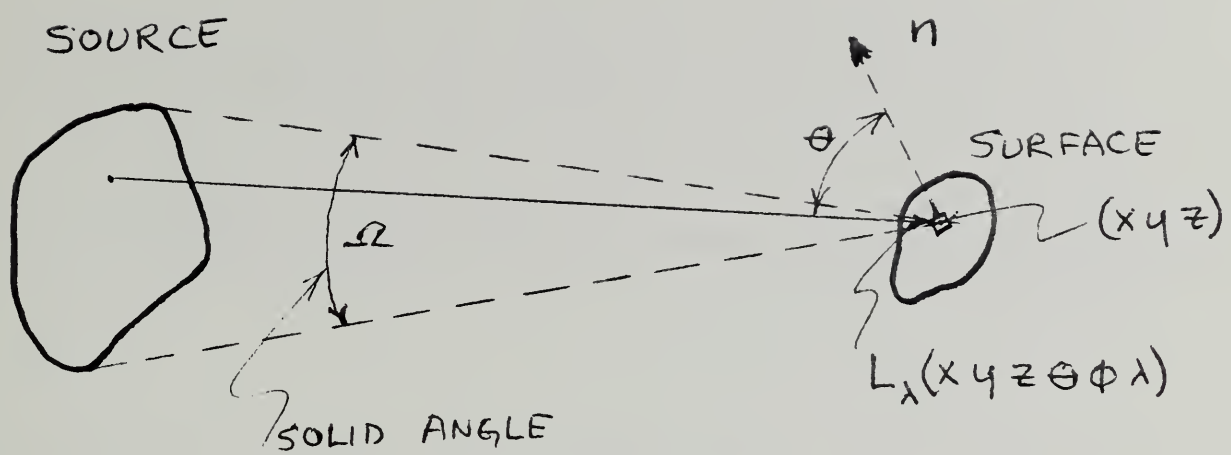

Fig. 18

Fig. 18 illustrates the geometry involved in Eq. (44) for the case of a source irradiating a surface where n is the normal to the surface at the point (xyz). The coordinate system used is similar to that employed previously with the polar axis coinciding with the surface normal. The solid angle Ω is the angle at the point (xyz) subtended by the source.

b. Determination of E_λ using a spectral irradiance standard

The simplest manner of determining spectral irradiance with a spectroradiometer is to consider the monochromator slit or field stop as the surface being irradiated. This means optics prior to the entrance slit of the spectroradiometer have to be removed. The output of the modified spectroradiometer when observing an unknown source of spectral

irradiance would then be

$$V(\lambda_o) = G\iiiiiii L_\lambda(x\,y\,z_o\,\theta\,\phi\,\lambda)\,dx\,dy\cos\theta\sin\theta\,d\theta\,d\phi\,\tau(x\,y\,\theta\,\phi)\mathcal{R}(x\,y\,\theta\,\phi)\,\sigma(\lambda_o\,\lambda)\,d\lambda \tag{45}$$

where zo refers to a point in the entrance slit or field stop, τ now excludes the preoptics, and the integrating limits, as before, cover the entrance pupil, entrance window and slit function. If τ and $\mathcal{R}$ are independent of $(xy\theta\phi)$

$$V(\lambda_o) = G\int_\lambda \tau\mathcal{R}\sigma\left\{\iint_{y\,x}\left(\iint_{\phi\,\theta} L_\lambda(x\,y\,z_o\,\theta\,\phi\,\lambda)\sin\theta\cos\theta\,d\theta\,d\phi\right)dx\,dy\right\}d\lambda \tag{46}$$

and if the solid angle subtended by the source at the slit is completely included in the entrance pupil,

$$V(\lambda_o) = G\int \tau\mathcal{R}\sigma\left\{\iint E_\lambda(x\,y\,z_o\,\lambda)\,dx\,dy\right\}d\lambda \tag{47}$$

where $E_\lambda(xyz_o\lambda)$ is the spectral irradiance at the point (xyz_o) in the entrance slit. Finally, if E_λ is independent of x and y

$$V(\lambda_o) = G\,A\int E_\lambda(z_o\,\lambda)\,\tau_\lambda(\lambda)\,\mathcal{R}_\lambda(\lambda)\,\sigma(\lambda_o\,\lambda)\,d\lambda \tag{48}$$

where A is the area of the entrance slit. Similarly, for the standard

$$V^S(\lambda_0) = G^S A \int \bar{E}^S_\lambda(z_0 \lambda)\tau_\lambda(\lambda)R_\lambda(\lambda)\sigma(\lambda_0 \lambda)\, d\lambda \qquad (49)$$

Eq. (48 and (49) are similar to Eqs. (20) and assuming τ and $\mathcal{R}$ are the same for the unknown and standard, the spectral irradiance can be obtained in the same manner as developed for spectral radiance.

Unfortunately, τ and $\mathcal{R}$ are rarely, if ever, independent of $(xy\theta\phi)$ and it is not uncommon for an error of 20% to be realized if this condition is assumed. This error can be significantly reduced by placing an optical element that diffuses the radiation in front of the detector as shown in Fig. 19.

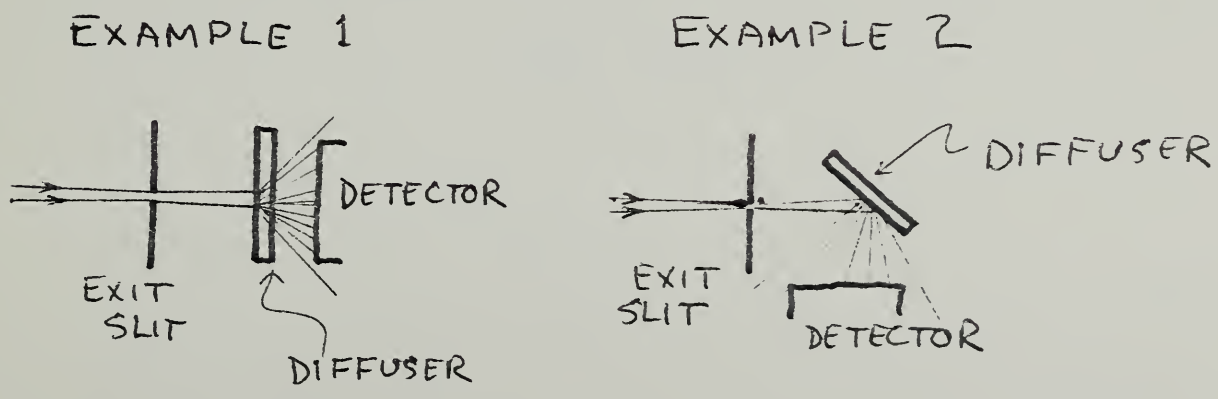

Fig. 19

This not only irradiates the entire receiving area of the detector but does this approximately uniformly tending to make $\mathcal{R}$ the same for both source and standard. This still leaves the error due to a non-uniform τ which can be particularly significant when the unknown and standard sources or beams are quite different.

A more accurate approach to a non-uniform τ and $\mathcal{R}$ is to make L_λ in Eq. (45) independent of $(xy\theta\phi)$. This can be accomplished by using an integrating sphere in front of the entrance slit as shown in Fig. 20.

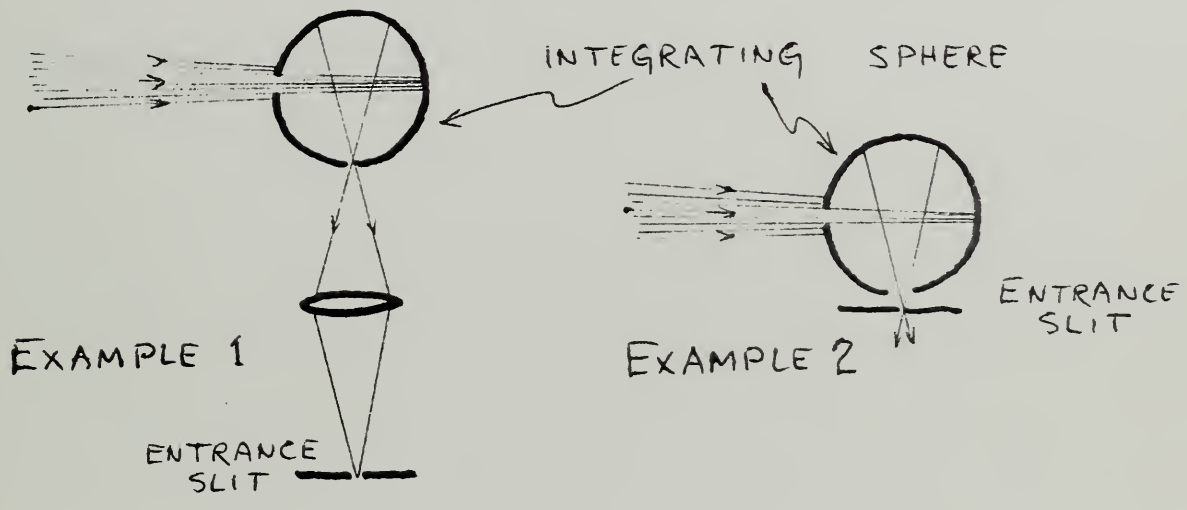

Fig. 20

Then

$$E_\lambda = K L_\lambda$$
$$E^s_\lambda = K^s L^s_\lambda \qquad (50)$$

and Eq. (45) becomes for the unknown and standard

$$V(\lambda_o) = \frac{G}{K}\int E_\lambda R_\lambda^e \sigma \, d\lambda$$
$$V^s(\lambda_o) = \frac{G^s}{K^s}\int E_\lambda^s R_\lambda^e \sigma \, d\lambda \qquad (51)$$

where E_λ and E_λ^s are the spectral irradiances at the entrance of the sphere. If the interior of the sphere is a uniform diffuse reflector and the sphere holes vanishingly small,

$$K = K^s \qquad (52)$$

and Eq. (51) can be used to accurately determine E_λ. Departures from uniformity and diffuseness in the reflectance of the sphere wall as well as the vanishingly small sphere holes can be compensated for by irradiating approximately the same area of the sphere wall by both the unknown and standard. A major limitation in this approach is that the sphere significantly reduces the flux incident on the monochromator and the corresponding reduction of the signal to noise ratio becomes a problem, particularly at short wavelengths.

c. Using a spectral radiance standard

If one wishes to determine the spectral irradiance of a source or

beam and is required to use a radiance standard, an arrangement similar to that shown in Fig. 20 is required when using the standard. The spectral irradiance at a point on the sphere opening is

$$E_\lambda^s(x\,y\,z_o\lambda) = \iint L_\lambda^s(x\,y\,z_o\theta\phi\lambda)\cos\theta\sin\theta\,d\theta\,d\phi \qquad (53)$$

where L_λ^s is now the spectral radiance at the sphere entrance. If $L_\lambda^s(xyz_o\theta\phi\lambda)$ is uniform relative to $(xy\theta\phi)$,

$$\bar{E}_\lambda^s = L_\lambda^s \pi \sin^2\theta \qquad (54)$$

and this can be used in Eq. (51). Small variations in L_λ^s relative to $(xy\theta\phi)$ can be taken care of by using an average spectral radiance, determined by the spectrometer, for an image similar to that entering the integrating sphere. To insure that Eq. (52) is valid, one should use an angle θ such that the sphere wall that is irradiated with the standard is as close as possible to that irradiated with the unknown irradiance. This can be checked experimentally by investigating the constancy of K^s as a function of θ in the relationship (obtained from Eqs. (50) and (54)

$$E_\lambda^s = L_\lambda^s \pi \sin^2\theta = K^s L_\lambda'$$

where L'_λ is the spectral radiance at the exit of the sphere.

d. Standards of spectral irradiance

The standards of spectral irradiance presently available in the U.S. are the 1000 watt General Electric Corporation type DXW or FBY tungsten halogen lamps. They are approximately 1 cm by 7.5 cm in size, are usually calibrated at 8.3 amperes, either AC or DC (approximately 110 volts), and are available from a number of commercial concerns with calibrations traceable to NBS. At the above current the spectral irradiance at 50 cm from the lamp is about 40 watts per cm^3 at 2500 nm, increases to about 250 at 1000 nm, and decreases to about 0.2 at 250 nm. The uncertainties currently assigned these lamps varies from about ±3% in the infrared to about ±8% in the ultraviolet. Since their stability for 100 hours of use is generally considerably better, an effort is being planned at NBS to try to reduce these uncertainties.

Recently, the irradiance of these standards has been significantly increased as a result of the development of a ceramic reflector to be used with the lamp (12). The new higher irradiance reflector type standards have an effective radiating surface of about 3 cm × 5 cm, and when used at a distance of 40 cm have about four times the spectral irradiance of the lamp (without a reflector) for wavelengths longer than 500 nm and about two times the irradiance at 300 nm. They are not calibrated below 300 nm because of the rapid change in the reflectance of the reflector at these short wavelengths.

REFERENCES

1. F. E. Nicodemus, Am. J. Phys. 31, 368 (1963).

2. A. C. Hardy and F. H. Perrin, The Principles of Optics, 68 (McGraw-Hill, New York, 1932).

3. H. J. Kostkowski and R. D. Lee, Temperature, Its Measurement and Control in Science and Industry, Volume Three, Part I, 449 (Reinhold Publishing Corp., New York, 1962).

4. H. J. Kostkowski and A. M. Bass, J. Quant. Spectrosc. Radiat. Transfer 1, 177 (1961).

5. J. C. DeVos, Physica 20, 690 (1954).

6. R. D. Larrabee, J. Opt. Soc. Am. 49, 619 (1959).

7. A. T. Hattenburg, Appl. Opt. 6, 95 (1967).

8. H. J. Kostkowski, D. E. Erminy, and A. T. Hattenburg, (High Accuracy Spectral Radiance Calibrations from 210 to 850 nm) In preparation, National Bureau of Standards, Washington, D.C. 20234.

9. W. H. Venable, Jr., (Effects upon Radiant Intensity Measurements due to Scattering in the Optical System) In preparation, National Bureau of Standards, Washington, D. C. 20234.

10. F. A. Jenkins and H. E. White, Fundamentals of Optics, 560 (McGraw-Hill, New York, 1957).

11. W. A. Shurcliff, Polarized Light, (Harvard University Press, Cambridge, Massachusetts, 1966).

12. W. E. Schneider, NASA Report, (Development of a High-Intensity Standard of Total and Spectral Irradiance) In preparation, National Bureau of Standards, Washington, D. C. 20234.

PART II

OPERATION, STABILITY AND CALIBRATION OF THE HIGH PRESSURE ARGON ARC

A. T. Hattenburg

SUMMARY

The spectral radiance and stability of the high pressure argon arc has been determined from 320 to 220 nm for the side-on, 50 ampere, 10 atmosphere pressure mode. The source produces a spectral radiance of about 8×10^5 to 17×10^5 watts/cm^3-sr over the wavelength region, and exhibits a stability of about ±0.2% per hour and 1% per 200 hours, with a signal to noise ratio of at least 1000.

This report presents details relative to the above results, the capabilities and limitations of the arc source, the methods of use and maintenance found desirable, and the apparatus and techniques utilized in this investigation. Also included is a preliminary study of the spectral irradiance of the arc.

SPECTRAL RADIANCE OF THE ARC SOURCE

a. Operating Parameters

The arc source is basically the same unit described in earlier reports (1,2), and a schematic diagram of it is shown in Fig. 1.* It was operated at a direct current of 50.15 amperes, an argon pressure of 150 psia, and argon exhaust flow rates of 4.5, 0.43, and 0.1

*The various components of the arc and auxiliary equipment discussed throughout this report are identified in Figs. 1 and 2.

liters/minute from the cathode, anode, and middle sections respectively. The argon was technical grade, quoted by the manufacturer as 99.996% pure. About nine liters/minute of 13 °C water was used for cooling. The spacing of the central plates was 1.0 mm and the channel diameter was 3.18 mm. For the major part of the investigation, the observed radiation emanated from a 0.6 mm wide by 0.8 mm high section at the center of the arc column, into a solid angle of 0.0028 sr. Earlier efforts employed a 0.1 mm by 0.8 mm target area.

b. Absolute values

The spectral radiance of one arc unit was determined over a period of 200 hours by comparison with a stable tungsten lamp, using the 0.6 by 0.8 mm target area. Values obtained at the seven chosen wavelengths are given in Table 1, and represent the spectral radiance emerging from a freshly cleaned quartz window.

Table 1. Spectral Radiance of Side-On 50 amp 150 psia Arc.

Wavelength (nm)	Spectral Radiance (w/cm^3 - sr)	No. of Determinations
320	16.8×10^5	15
300	15.6	3
280	14.2	3
260	12.6	7
240	10.5	3
225	8.5	4
220	7.6	15

The radiation is unpolarized, and except for the carbon line at 247.8 nm, contains no spectral lines from 200 to 335 nm.

The estimated standard deviation uncertainties of these absolute values are 2% at 320 nm increasing to 4% at 220 nm. Standard deviations of the individual measurements were about 1% throughout the wavelength region.

Another set of determinations on another arc unit were obtained earlier over a 100 hour period. In this case a graphite arc was used as the reference standard (3) with a target area of 0.1 by 0.8 mm. The observed values, when adjusted to the 0.6 mm target width, were lower than those of Table 1 by about 6% throughout the wavelength range. The estimated standard deviation uncertainties of these absolute values are 3% at 320 nm and 6% at 220 nm and standard deviations of the individual measurements varied from about 2% at the longer to 4% at the shorter wavelengths.

c. Short term stability and noise

The spectral radiance of the arc typically varies by less than 0.2% over one hour periods, when operated from the constant current power supply. The signal to noise ratio is about 1000, when measured with a one second time constant system and the spectroradiometer described in an earlier report (1).

d. Long term stability

The spectral radiance of the arc remained constant over the 200 hour period, within the 1% precision of the measurements. About 15 determinations were made at both 320 and 220 nm. The same result is obtained, within the 2 to 4% precision, from the 100 hours of graphite arc comparisons, when the data is adjusted for the estimated decrease in transmittance of the undisturbed quartz window.

e. Quartz window transmission

The measured transmittance of the quartz window varied smoothly from about 0.91 at 320 nm to 0.82 at 220 nm. The transmittance remained constant, within the measurement precision, when the window was cleaned daily. When used without cleaning for periods of about 50 hours, the relative transmittance decreased by 0.025% per hour at 320 nm and 0.06% per hour at 220 nm.

f. Geometric stability

Repeated observations on the selected volume of the arc stream indicated that the arc column is spatially stable to better than 0.05 mm. Repeated scans over the column width and height (between the central constricting plates) indicated a repeatability in position of the radiation peak of about 0.03 mm. Measurements of the radiation half-width (width of the arc column at the half-radiance points) over the 200 hours yielded values between 1.63 and 1.69 mm.

g. Positioning sensitivity

The decrease in radiance output of the arc when moved from the normal viewing position (radiation maximum) by 0.02 mm, either parallel or normal to the column axis, is undetectable. Changes of 0.1 mm result in a decrease of almost 1%.

h. Sensitivity to changes in operating parameters

The spectral radiance of the arc is most sensitive to changes in the operating current and argon pressure. An increase or decrease of 0.5% (0.25 amperes) in current or 2% in absolute pressure causes a corresponding increase or decrease of about 1% in spectral radiance. The power supply typically holds the current to within ±0.05% of the set value over an 8 hour period; the absolute pressure decreases about 0.5% per hour without adjustment.

The spectral radiance is at a minimum for the chosen argon flow rate in the cathode region, so that either an increase or decrease of 24% in this flow causes a 1% increase in radiance. The influence of the exhaust flow rates from the middle and anode regions is negligible, amounting to less than a 0.1% change in radiance for a 50% change in flow.

Raising the temperature of the cooling water from 13 °C to 25 °C or lowering its flow rate from 9 to 5 liters/minute caused an increase in spectral radiance of about 0.1%.

i. Suitability of the arc as a standard source

The results of this investigation establish the value of the arc as a stable, intense standard source of spectral radiance in the near ultraviolet, when the arc is calibrated as an individual unit. When components are changed or a completely new unit is used (1) radiance changes varying from zero to 14% have been observed. Thus, for optimum results, each arc unit must be individually calibrated. However, experience with the arc components fabricated with the most recent vacuum brazing techniques (see appendix) suggests that a unit should operate stably for at least a few hundred hours, and probably significantly longer, without requiring replacement of components and therefore recalibration.

OPERATION OF THE ARC

a. Design changes

The arc used in this investigation and shown in Fig. 1 is basically the same model described earlier (1,2). Slight modifications which have evolved during this study include the replacement of the electronic ripple filter with a more simple filter composed of an array of inductors and capacitors, a starting resistor used to prevent high transient currents when striking the arc (see electrical circuit in Fig. 2), warning buzzers which signal the absence of cooling water, an arc mount allowing more

precise orientation of the unit, and the improved method of vacuum brazing the constriction plates (see appendix).

b. Alignment of the arc

Before initial operation of the arc, a mechanical alignment is performed, utilizing small aperture inserts in place of the front and rear windows. The apertures, consisting of a 2 mm hole in a circular plate, are illuminated from the rear with a strong light, and the unit is oriented until the images of the apertures are aligned on the entrance slit. The inserts are then removed, a close-fitting rod is inserted in the arc channel, and the arc translated until the edges of the rod are focused and centered on the slit.

c. Preliminary steps

Before preparing to start the arc, the front quartz window should be removed and cleaned.* The length of the tungsten cathode should be measured, and adjusted if it has deviated by more than 0.3 mm from its optimum length of 1.25 mm projection from the hollow graphite cathode (see Fig. 1). The resistances between the cathode, successive constriction plates and anode should be measured to detect any shorting in

*In this investigation the cleaning solutions employed were either ethyl alcohol or aerosol soap, followed by distilled water rinsing and drying.

the system, due to large water leaks or other causes. These measurements are made with cooling water applied, and typical values are 0.5 to 2.0 megohms.

d. Starting and stopping procedure

The cooling water is turned on, the argon exit flow valves are opened slightly, and a slight flow of argon is induced in the arc by adjusting the inlet regulator pressure (large initial flows result in formation of a plasma jet at the hollow cathode). The shorting switch for the 3.5 Ω starting resistor is opened, and power applied to the electric supply unit. The DC voltage is raised to about 150 volts, and the arc is ignited with the brass starting rod. Starting current is about 20 amperes. The tungsten cathode is lowered into place and the cap tightly fastened. The starting resistor is shorted, raising the current to about 40 amperes, the argon pressure brought to 150 psia, and the flow rates adjusted. The DC voltage is raised and the bias control setting adjusted until the arc has reached the operating current and the voltage across the current regulator attains some selected value between 15 to 30 volts. After a short wait to allow all components to reach equilibrium (5-10 min.) the arc is ready for use.

When extinguishing the arc, the DC voltage is lowered to zero, input power shut off, and water and argon supplies shut down. If immediate adjustments or dissembly of the arc is attempted, the water and argon

should be bled from the system, and the residual charge on the capacitors removed.

If the flow rate valves and bias control setting are left undisturbed, only minor adjustments will be required for the flows in subsequent starts, while the electric current will be set by simply raising the DC voltage until the chosen value appears across the current regulator.

e. Operating procedures

With the arc operating under standard conditions, the final alignment procedure is undertaken. Radiometric scans through the rotational degrees of freedom are made to insure that the peak radiance is being observed. The arc is carefully adjusted in the directions parallel and perpendicular to the column axis (leaving focus undisturbed), until the maximum radiation output is also obtained relative to these degrees of freedom. This procedure is repeated each time the arc is returned to the viewing position after observations on another source. The argon flow rates are set and the current measured at the time of each radiance reading if optimum accuracy is desired.

The image of the arc column and surrounding constriction plates should be examined periodically for any evidence of foreign material in the chamber or spatial instability in the column. These problems may often be cured by temporary large increases of argon flow in the various sections. Instability of current or radiance output may often

be overcome by choosing a slightly different voltage drop across the current regulator.

CALIBRATION METHODS

The high pressure arc was calibrated against known standards of spectral radiance by means of the high accuracy spectroradiometer, utilizing the ratio of amplified output currents of the detector to obtain radiance ratios. Two methods of calibration were employed. The first consisted of a direct comparison of the high pressure arc with the low current graphite arc (3) over a period of 100 hours of operation. The limited precision of this method, due to short-term fluctuations in the graphite arc, dictated a new approach. The second method consisted of comparing the arc radiance, as viewed through a set of calibrated filters, with that of a very stable quartz-windowed tungsten strip lamp. This approach was employed during a 200-hour test to determine the long term stability of the arc.

a. Details of the calibration

The calibration methods involved comparisons between sources of different spectral distribution, size, strength, and uniformity. It was therefore necessary to investigate the possible errors arising from these factors, as described in Part I of this report, "The Principles and Methods of Calibrating Spectroradiometers".

The spectroradiometer employs a double monochromator with a tri-alkali photomultiplier detector, equal entrance and exit slits, and an

optical magnification of one. For the 0.6 mm slits used here, the measured slit function exhibits a transmission in the distant wings on the order of 10^{-9}, with a resulting error of less than 0.1% due to spectrally scattered light. The effective spectral response was found to be independent of the flux magnitude. The "size of source" effect was determined to be less than 0.1% for the sources employed here. Placement of the detector 15 cm from the exit slit reduced the effect of non-uniform source areas to negligible amounts. All sources used here were found to be uniform over the solid angle utilized, and to have negligible polarization. The detector-amplifier response was calibrated for the range of signal ratios employed (3), and corrections applied to each measured ratio.

b. Calibration with graphite arc standard

Comparisons with the graphite arc were made at five wavelengths from 320 to 210 nm, over a period of 100 hours. From eleven to eighteen determinations were made at each wavelength. The slit was set at 0.1 mm width and a mask was used to obtain a 0.8 mm height, resulting in a spectral bandpass of 0.15 nm at 210 nm increasing to 0.25 nm at 320 nm. The solid angle was restircted to 0.0028 sr by an external circular stop. All comparisons were made at fixed wavelengths.

The low current graphite arc was operated in the standard manner (3), with the current just below the overload point and the central

portion of the anode focused on the slit. Each anode was burned for ten minutes before readings were taken, and five minutes was allowed when anodes were reignited. Nine anodes were consumed during this period, and comparisons at a given wavelength were repeated for a majority of the anodes.

The comparisons were made at each wavelength with the graphite arc anode being centered on the slit, and the high pressure arc image peaked for maximum signal. Checks and adjustments of the operating parameters of each source were made while the other source was being observed. A determination consisted of one or more readings of the high pressure arc over a one minute time span, each surrounded by similar readings of the graphite arc. The ratio of spectral radiance at that wavelength was then derived from the output currents of the photomultiplier, with appropriate corrections for non-linearity of the detector-amplifier response. The quartz window was left undisturbed for 70 hours of operation, and cleaned frequently thereafter. Any effect on the radiance output of the arc due to this cause was not detectable within the precision of the method. During the latter part of the 100 hour period, water leaks appeared in various sections of the arc, necessitating replacement of these sections. This led to the development of the vacuum brazing technique described in the appendix for fabricating new components for the arc.

c. Calibration with tungsten strip lamp and filters

The high pressure arc was compared to the tungsten strip lamp at seven wavelengths from 320 to 220 nm over a period of 200 hours. About fifteen determinations were made at 320 and 220 nm, and three to six at the remaining wavelengths. The slit was set for a 0.6 mm width and masked to a 0.8 mm height, resulting in a spectral bandpass of 1.0 nm at 220 nm and 1.5 nm at 320 nm. For the determination of the radiance width of the arc, the slit was narrowed to 0.05 mm. The solid angle remained at 0.0028 sr.

The spectral radiance of the tungsten lamp was determined during the course of the arc studies to an estimated uncertainty of about 1.5% (1). The orientation and positioning of the lamp is routinely accomplished to a precision of about 0.1%.

The spectral radiance of the high pressure arc exceeded that of the lamp by a factor varying from about 10^3 at 320 nm to 10^5 at 220 nm, making direct comparisons of the two sources impractical. A set of commercially available neutral transmission filters was used to attenuate the arc output. The filters were composed of a sandwich of two pieces of ultraviolet transmitting quartz, with an inconel metal film deposited on the inner faces, and had nominal transmittances of 10%, 1%, and 0.1%. Wedges were inserted between the edges of the quartz plates in order to form a slight angle between the metallic surfaces, thereby diverting

from the optical path the secondary images which arose from internal reflections. When used with the arc in pairs, the filters were mounted at a two degree angle from one another to avoid similar reflections.

The comparisons were made at each wavelength with the lamp image being precisely located on the slit, and the image of the arc, with appropriate filters mounted, peaked for the maximum signal. The radiance ratios were derived from the detector currents and the measured filter transmittances, with corrections for the non-linear response. The radiance width of the arc was then determined at 320 nm. During the last 150 hours, the filters were calibrated immediately after each set of source comparisons.

d. Filter calibrations

The filters were calibrated in situ using the arc as reference source. It was necessary to adjust the arc position for each filter insertion, due to image shifting caused by mounting the filters at angles to the normal. At each wavelength, the 10% filter was calibrated by alternately inserting and removing it from the output beam of the arc, with appropriate changes in amplifier gain. The ratio of detector currents, corrected for nonlinearity, yielded the transmittance. Filters of lower transmittance were calibrated by comparison to the 10% filter, in order to avoid uncertainties from large ratios of detector current.

The effect of heating upon filter transmittance was investigated by alternating nearly identical filters, with long exposures to allow

for any heating effects. Comparisons were also made between sets of filters calibrated singly and used in pairs. In both cases no effects were observed within the precision of the measurements.

The transmittance of the quartz window was determined by using a replacement window in the arc unit, and mounting the regular window as near as possible to its normal position in the arc beam.

SPECTRAL IRRADIANCE EVALUATION

A preliminary evaluation of the spectral irradiance of the 50 ampere 150 psia arc was obtained by comparison with a 1000 watt tungsten-iodide quartz lamp (4) calibrated for spectral irradiance down to 250 nm. The two sources were alternately positioned on the optic axis of the monochromator, about one meter from the 0.6 mm wide by 0.8 mm high entrance slit. The spectral irradiance of the arc at one meter was found to be 4.3, 3.7 and 2.7 watts/cm^3 at wavelengths of 320, 280, and 250 nm respectively, to an estimated accuracy of about 15%. In the lower region where no calibration was available, the arc spectral irradiance exceeded that of the lamp by factors of 80 at 240 nm to 500 at 210 nm. The arc irradiance at 250 nm remained stable to about 0.2% over half-hour periods, and repeated to better than 0.5% when extinguished and relit.

The present limitations in the wavelength and accuracy of currently available spectral irradiance standards preclude a significantly more accurate calibration of arc irradiance at this time. A major effort

to improve and extend (in wavelength) these standards is being undertaken, utilizing the existing high accuracy spectral radiance standards, small-aperture integrating spheres (compatible with the small target areas of these sources), and low-level detection techniques, required because of the resulting low ultraviolet flux levels. When completed this work is expected to permit a more accurate and extensive evaluation of the arc as a source of spectral irradiance.

REFERENCES

1. H. J. Kostkowski, C. R. Yokley, D. E. Erminy, and A. T. Hattenburg, NBS Report 9099, (1965).
2. C. R. Yokley, Proceedings, International Symposium on Solar Radiation Simulation, Jan. 18-20, 1965, Institute of Environmental Sciences.
3. A. T. Hattenburg, Appl. Opt. 6, 95 (1967).
4. R. Stair, W. E. Schneider, and J. K. Jackson, Appl. Opt. 2, 1151 (1963).

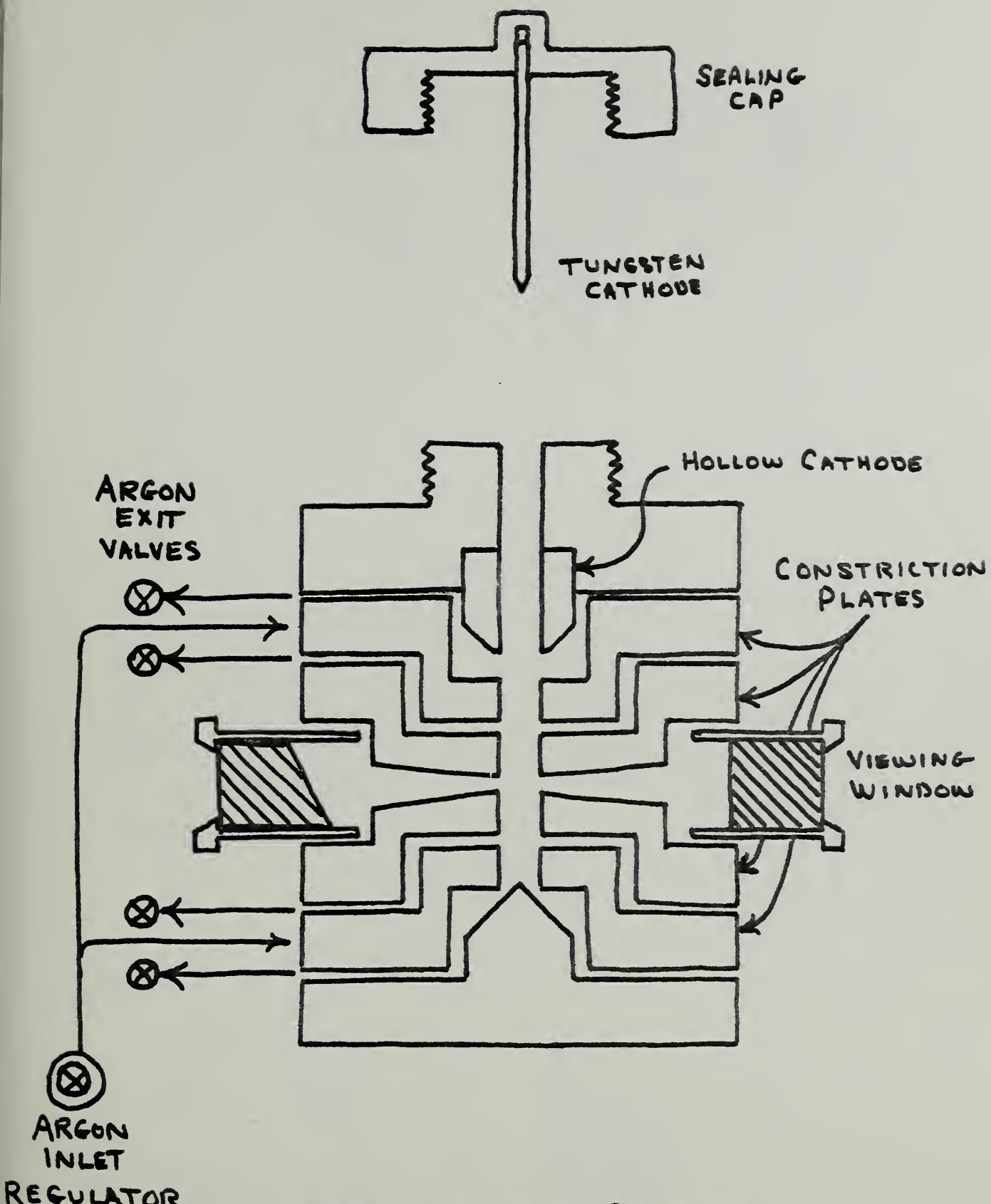

FIG. 1. ARC SCHEMATIC.

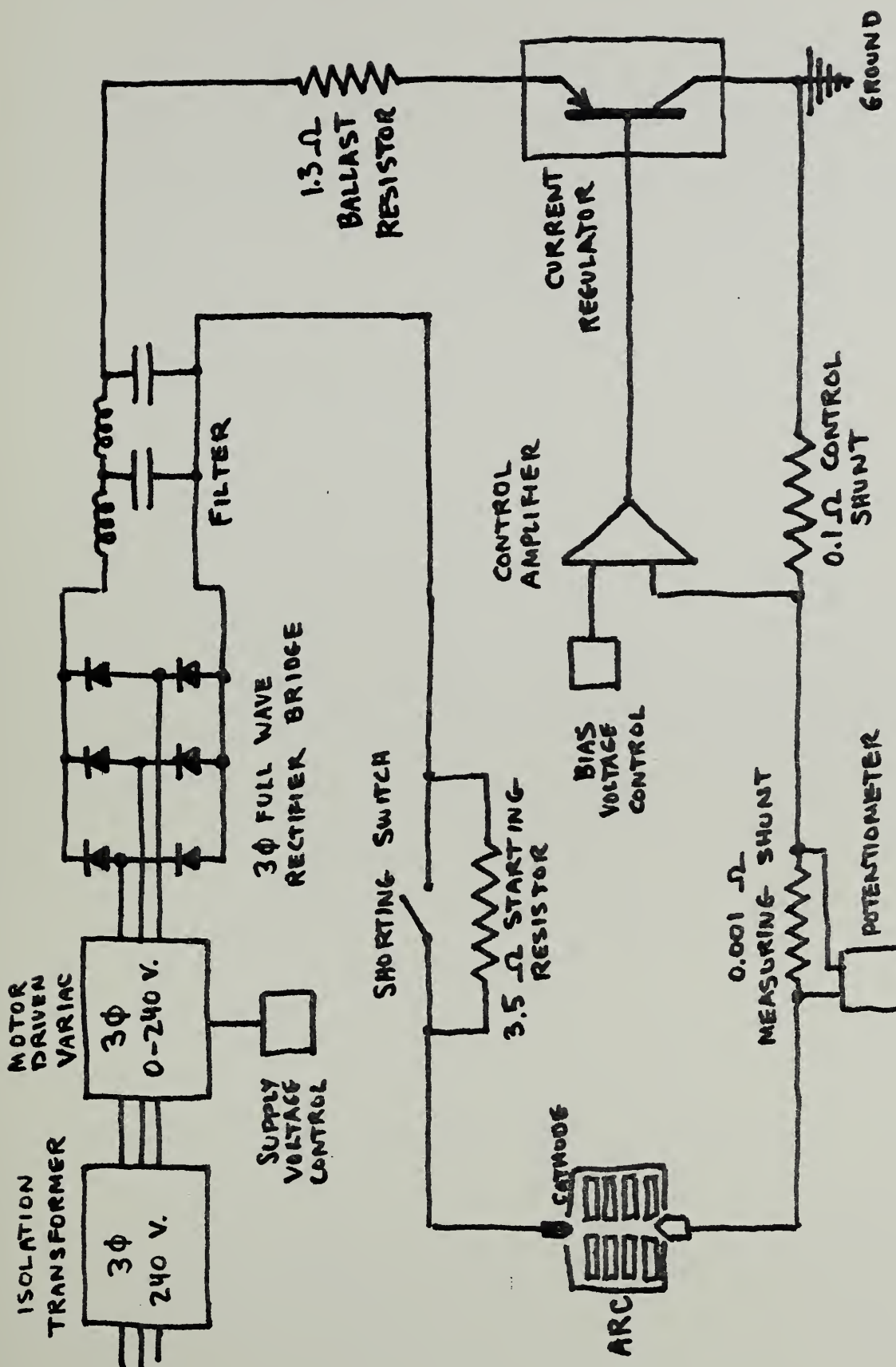

FIG. 2. ELECTRICAL CIRCUIT

APPENDIX

a. Fabrication of constriction plates

An improved method of fabrication of the constriction plate sections of the arc became necessary, due to frequent occurrence of water leaks at the silver soldered copper-stainless steel joints. Inspection of the defective components disclosed poor adherence of the solder to the stainless steel surfaces, and presence of oxide films in part of the joints. Efforts to repair the defective components by cleaning and resoldering the joints were unsuccessful. Soldering in an inert atmosphere, with or without flux, also failed to achieve tight joints.

A successful method of forming tight joints by vacuum brazing was developed, and components fabricated by this method have remained leak-proof for over a 100 hours of hydrostatic tests and 200 hours of operation as arc components. The design of the units was altered to increase the contact area between the stainless steel and copper by about a factor of 5. After being machined, the parts are degreased and electro-polished. Inserts of a special gold-nickel alloy* are placed between the parts to be joined, and the unit is heated in a vacuum furnace at about 30 microns until the alloy melts.

*NIORO alloy. Western Gold & Platinum Company, Belmont, California.


DEPARTMENT OF COMMERCE
NATIONAL BUREAU OF STANDARDS